



Research paper

Synthesis, molecular docking and biological evaluation of novel phthaloyl derivatives of 3-amino-3-aryl propionic acids as inhibitors of *Trypanosoma cruzi* trans-sialidase

Muhammad Kashif^a, Karla Fabiola Chacón-Vargas^b, Julio Cesar López-Cedillo^b, Benjamín Noguera-Torres^b, Alma D. Paz-González^a, Esther Ramírez-Moreno^c, Rosalia Agusti^{d,e}, Maria Laura Uhrig^{d,e}, Alicia Reyes-Arellano^f, Javier Peralta-Cruz^f, Muhammad Ashfaq^g, Gildardo Rivera^{a,*}

^a Laboratorio de Biotecnología Farmacéutica, Centro de Biotecnología Genómica, Instituto Politécnico Nacional, 88700, Reynosa, Mexico

^b Departamento de Parasitología, Escuela Nacional de Ciencias Biológicas, 07320, Ciudad de México, Mexico

^c Escuela Nacional de Medicina y Homeopatía, Instituto Politécnico Nacional, 07320, Ciudad de México, Mexico

^d Universidad de Buenos Aires, Facultad de Ciencias Exactas y Naturales, Departamento de Química Orgánica, Pabellón 2, Ciudad Universitaria, C1428EG, Buenos Aires, Argentina

^e Consejo Nacional de Investigaciones Científicas y Técnicas (CONICET)-UBA, Centro de Investigaciones en Hidratos de Carbono (CIHIDECAR), Buenos Aires, Argentina

^f Departamento de Química Orgánica, Escuela Nacional de Ciencias Biológicas, 07320, Ciudad de México, Mexico

^g Department of Chemistry, The Islamia University of Bahawalpur, Bahawalpur, Pakistan

ARTICLE INFO

Article history:

Received 7 June 2018

Received in revised form

2 July 2018

Accepted 3 July 2018

Available online 7 July 2018

Keywords:

Trans-sialidase

Trypanosoma cruzi

Molecular docking

Propionic acid

Phthaloyl

Inhibitors

ABSTRACT

In the last two decades, trans-sialidase of *Trypanosoma cruzi* (TcTS) has been an important pharmacological target for developing new anti-Chagas agents. In a continuous effort to discover new potential TcTS inhibitors, 3-amino-3-arylpropionic acid derivatives (series A) and novel phthaloyl derivatives (series B, C and D) were synthesized and molecular docking, TcTS enzyme inhibition and determination of trypanocidal activity were carried out.

From four series obtained, compound D-11 had the highest binding affinity value (−11.1 kcal/mol) compared to reference DANA (−7.8 kcal/mol), a natural ligand for TS enzyme. Furthermore, the 3D and 2D interactions analysis of compound D-11 showed a hydrogen bond, π - π stacking, π -anion, hydrophobic and Van der Waals forces with all important amino acid residues (Arg35, Arg245, Arg314, Tyr119, Trp312, Tyr342, Glu230 and Asp59) on the active site of TcTS. Additionally, D-11 showed the highest TcTS enzyme inhibition (86.9% \pm 5) by high-performance ion exchange chromatography (HPAEC). Finally, D-11 showed better trypanocidal activity than the reference drugs nifurtimox and benznidazole with an equal % lysis (63 \pm 4 and 65 \pm 2 at 10 μ g/mL) and LC₅₀ value (52.70 \pm 2.70 μ M and 46.19 \pm 2.36 μ M) on NINOA and INC-5 strains, respectively. Therefore, D-11 is a small-molecule with potent TcTS inhibition and a strong trypanocidal effect that could help in the development of new anti-Chagas agents.

© 2018 Elsevier Masson SAS. All rights reserved.

1. Introduction

Chagas disease affects 8 to 10 million people worldwide, primarily in South and Central America [1–3]. Only two approved drugs, nifurtimox (Nfx) and benznidazole (Bzn), are currently used

in the world and have been for the last four decades; however, both drugs display low efficacy in the chronic phase of infection and are associated with severe undesirable side effects [4–9]. Currently, Trans-sialidase of *Trypanosoma cruzi* (TcTS), a non-homologous enzyme in humans or hosts, which is mainly expressed by trypanomastigotes, has been reported by various research groups as a pharmacological target for Chagas disease. This enzyme catalyses the transfer of sialic acid from the host glycoconjugate surface to the *Trypanosoma cruzi* (*T. cruzi*) mucin-like glycoprotein surface and

* Corresponding author. Centro de Biotecnología Genómica, Instituto Politécnico Nacional, Boulevard del Maestro, s/n, Esq. Elías Piña, 88710, Reynosa, Mexico.

E-mail addresses: gildardors@hotmail.com, giriveras@ipn.mx (G. Rivera).

also helps *T. cruzi* escape from the host immune system [10–12].

The kinetic, structural, molecular docking, quantum mechanical/molecular mechanical (QM/MM) molecular dynamics (MD) simulation analysis of TcTS enzyme has provided evidence that the residues Arg35, Arg245, Arg314, Asp59, Glu230, Trp120, Trp312, Tyr119, Tyr342, Val95 and Leu176 play a key role in transferring sialic acid, in stabilizing the transition states and in accommodating the lactosyl moiety to the donor/acceptor substrates. Furthermore, the aromatic residues contribute to the formation of a hydrophobic pocket in the enzyme catalytic cavity [10,11,13,14].

In addition to rational drug design, *in silico* screening methodology has been adopted to find a strong (non-sugar based) TcTS inhibitor. For example, Neres et al., in 2007 and 2009, using an *in silico* screening, found some compounds with novel scaffolds (non-sugar benzoic acid and pyridines derivatives), with submillimolar IC_{50} values (Fig. 1 and 1–4) [15,16]. Later, the virtual screening of a natural product library by Kim et al. (2009) and Arioka et al. (2010) showed that quinolinone and flavonoid derivatives (Figs. 1, 5 and 6) are the most potent compounds with sub-micromolar TcTS inhibition values [17,18].

In the search for new non-sugar based inhibitors of TcTS, we propose the synthesis of 3-amino-3-arylpropionic acid derivatives (series A) due to the presence of NH_2 and $-COOH$ groups, which could enhance the ability to interact with amino acid residues in the catalytic cavity of TcTS [19]. Additionally, novel phthaloyl derivatives of 3-amino-3-arylpropionic acid (series B, C and D) were proposed from 3-amino-3-arylpropionic acid derivatives (series A) (Scheme 1) to enhance more interaction on the active site of TcTS due to the presence of a carbonyl group on the phthaloyl moiety. Our main focus was to propose compounds that could bind to the TcTS residues, a) Asp59, Glu230 and Tyr342, which are involved in stabilizing the transition state by protonation and deprotonation during sialic acid transfer; and b) Trp312 and Tyr119, which are hydrophobic in nature and are present at the mouth of the catalytic cleft and that control substrate entry in the catalytic pocket. Also, a phthaloyl/phthalimide structural framework could enhance hydrogen bonding and π - π stacking interaction on TcTS active

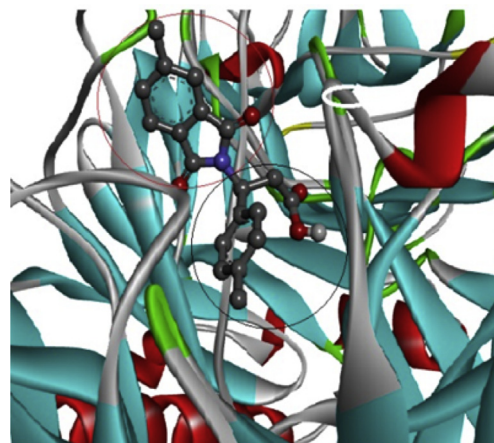


Fig. 2. The orientation of phthaloyl derivatives of 3-amino-3-arylpropionic acid inside the TcTS catalytic cavity (ribbons showing TcTS enzyme 1MS8). The red circle shows the phthaloyl group at the mouth of the cavity and the black circle shows 3-amino-3-arylpropionic acid deep inside the cavity. The 3D image was produced by Discovery studio visualizer R-2 client 2017 version. (For interpretation of the references to colour in this figure legend, the reader is referred to the Web version of this article.)

residues due to a carbonyl group and aromatic ring moiety, respectively. Furthermore, phthaloyl/phthalimide derivatives have also received great attention due to their COX-1/2 inhibition [20], anti-inflammatory [21], antihyperlipidemic [22], antitumor/anticancer, anxiolytic, analgesic [23–26], antimicrobial, anticonvulsant, antitubercular [27–29], antipsychotic [30], antiproliferative [31], immunomodulatory [32], antiangiogenic [33], schistosomicidal [34] and anti-protozoa (anti-trypomastigotes) activities [35]. All the compounds proposed were analyzed by molecular docking on the active site of TcTS using Auto Dock Vina 4.0. Furthermore, the TcTS enzyme inhibition assay of selected compounds and *in vitro* anti-*T. cruzi* activity on trypomastigotes of NINOA and INC-5 strains were also evaluated.

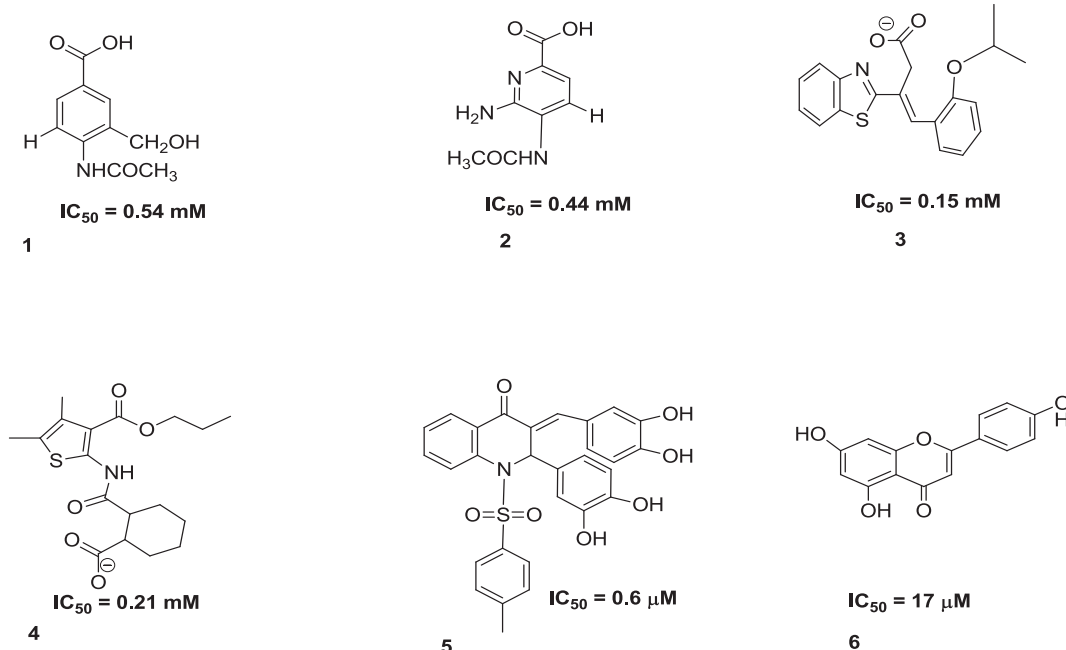


Fig. 1. Structure and inhibition values for representative known TcTS non-sugar based inhibitors obtained from molecular docking and virtual screening of a chemical library.

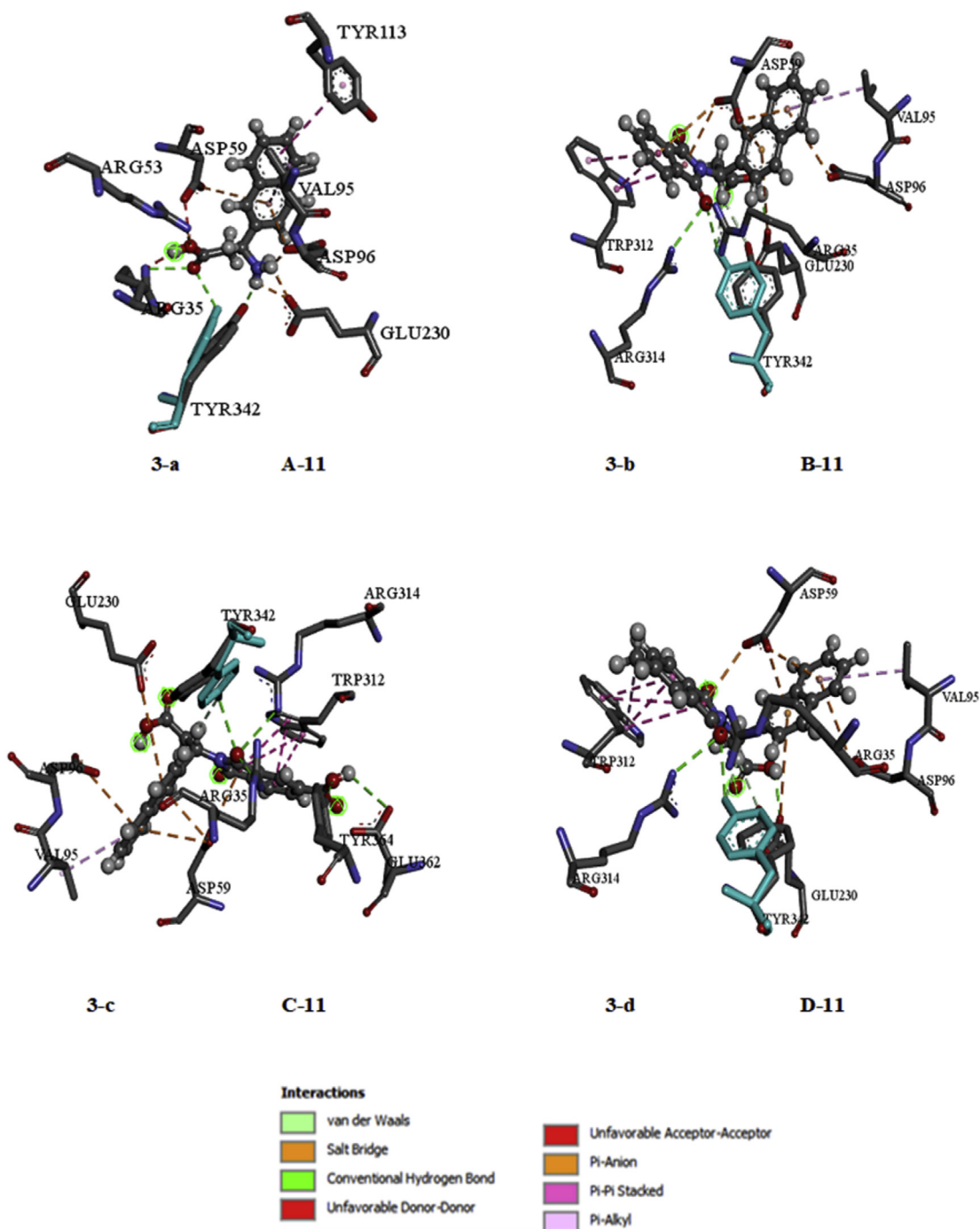


Fig. 3. 3D interaction of compounds with the highest predicted binding affinities: 3-a (series A, compound A-11), 3-b (series B, compound B-11), 3-c (series C, compound C-11) and 3-d (series D, compound D-11) compared to the reference DANA (-7.8 kcal/mol). The 3D image was produced by Discovery studio visualizer R-2 client 2017 version.

2. Results and discussion

2.1. Chemistry

Compounds from series A, B, C and D were synthesized according to [Scheme 1](#). Series A is described as 3-amino-3-arylpropionic acid derivatives and were synthesized following the procedure reported in the literature [36]. The phthalic anhydride (series B), trimellitic anhydride (series C) and 4-methylphthalic anhydride (series D) phthaloyl derivatives of 3-amino-3-

arylpropionic acid were synthesized by the fused reaction as described in the experimental section [37].

The FTIR spectra of series A, showed a broad $-OH$ peak in the range of $3300-2900$ cm^{-1} and the absence of a $-NH_2$ peak due to an interchangeable hydrogen atom between $-OH$ and $-NH_2$. Also, carbonyl ($C=O$) peaks in $1650-1600$ (short) cm^{-1} confirmed the synthesis. Furthermore, the 1H NMR showed the peak in the range of the chemical shift $4.60-4.40$ (singlet) ppm due to an interchangeable hydrogen atom between $-OH$ and $-NH_2$, which also confirmed the synthesis.

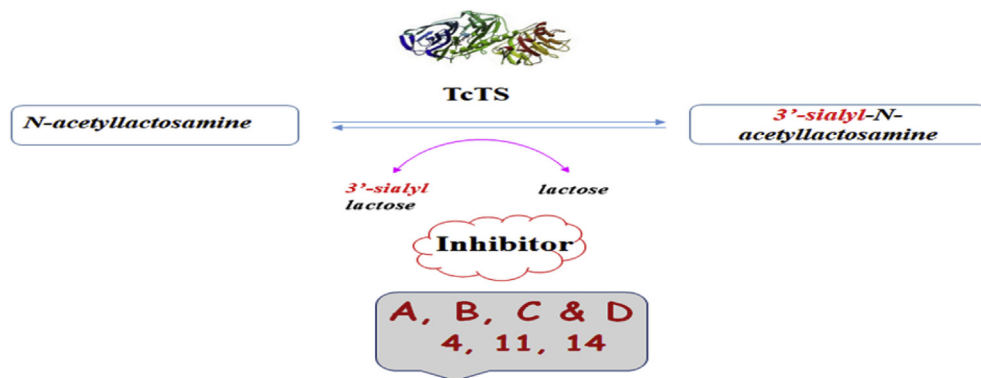


Fig. 4. Sialylation of *N*-acetyllactosamine catalyzed by TcTS as a target of the inhibitors tested.

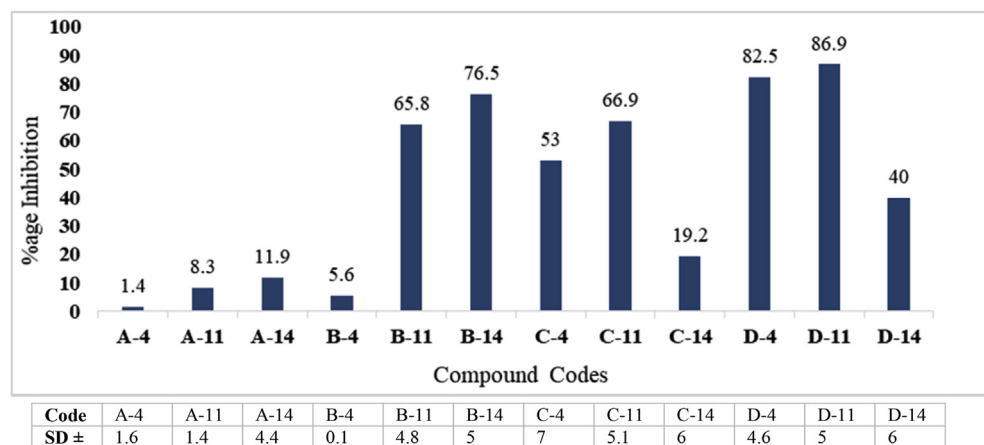


Fig. 5. Percentage inhibition of TcTS enzymes by selected compounds of series (A–D), determined by HPAEC-PAD. Each compound was tested in triplicate ($n = 3$).

The phthaloyl derivatives of 3-amino-3-arylpropionic acid (series B, C and D) were confirmed by FTIR, phthalimide peaks in the range of C_2O_2N (phthalimido): 1770 asymmetric, 1690 symmetric cm^{-1} and a carbonyl ($C=O$) peak in the range of 1650–1610 cm^{-1} . The $-OH$ proton peak of the carboxylic acid of the 3-amino-3-arylpropionic acid part in 1H NMR was found in a range of 13.20–11.90 ppm and a singlet proton peak of $CH-N$ of phthalimide in a range of 5.80–5.30 ppm, which also strengthened the synthesis of compounds.

2.2. Molecular docking analysis

The 3-amino-3-arylpropionic acid derivatives with different substituents were used as a starting point to propose TcTS inhibitors due to the presence of $-NH_2$ and $-COO^-$ groups, which could help to show inhibitory effects. The substituents (1–15) were categorised according to their chemistry as electron donating substituents ($-OCH_3$, $-CH_3$, and $-C_2H_5$), electron withdrawing substituents (OH , NO_2 , $-F$, $-Cl$, Br , and $C_2H_2O_2-mNO_2$), aromatic substituents (naphthyl and biphenyl) and heterocyclic moieties (furanyl and thienyl) to understand the effects of these modifications on TcTS binding sites, enzyme inhibition and trypanocidal activity.

To increase the interaction of 3-amino-3-arylpropionic acid derivatives (series A) on the TcTS active site, their novel phthaloyl derivatives were proposed by coupling them with phthalic anhydride (series B), trimellitic anhydride (benzene-1,2,4-tricarboxylic anhydride) (series C) and 4-methylphthalic anhydride (series D).

When these phthaloyl derivatives were sketched in 3D and their energy minimized, these compounds showed a chair-shaped geometry, and when they were fitted in TcTS catalytic cavity, it was found the 3-aryl propionic acid skeleton deep inside the catalytic cavity with the carboxylic group flipped near to the active amino acid residues Arg35, Arg245, Arg314, Asp59, Glu230 and Tyr342.

On the other hand, the phthaloyl group was found at the mouth of the TcTS catalytic pocket with a carbonyl group near the key amino acid residues Tyr119 and Trp312. To produce a stronger interaction, the hydrophilic $-COOH$ and hydrophobic $-CH_3$ substituents at 4-position on the phthaloyl ring were also considered. To understand the binding mode of the enzyme with molecules, 3-aryl propionic acid and the phthaloyl moiety were considered separately (Fig. 2).

To understand and establish the interaction of the proposed molecules with key amino acid residues on the catalytic pocket of TcTS (PDB code 1MS8), molecular docking studies were performed to explore the best predicted binding affinities. The TcTS natural ligand 2-deoxy-2,3-didehydro-*N*-acetylneuraminic acid (DANA) was used as a reference obtaining a predicted binding affinity value of -7.8 kcal/mol.

From series A (Table 1), only six compounds showed predicted binding affinities that were the same (A3 and A5) or better (A-9 to A-12) than the reference DANA (-7.8 kcal/mol). The compounds A-3 and A-5 only bind the two amino acid residues Arg35 and Tyr342 via conventional hydrogen bonding, while Asp96 and Glu230 showed salt bridge interaction. Also, compound A-5 showed an unfavourable interaction with Arg53 and Asp59; in contrast, Glu230 was bound

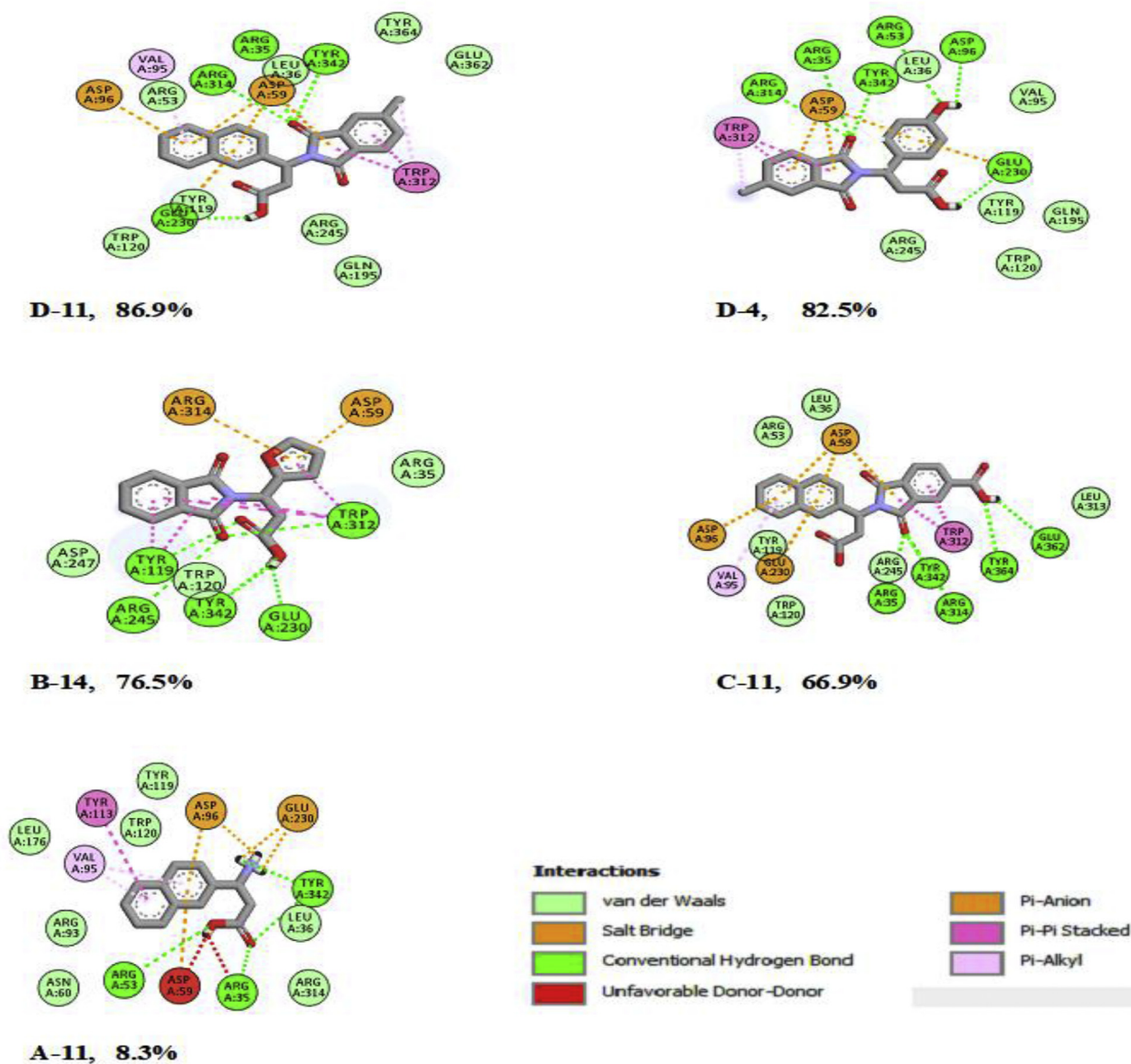
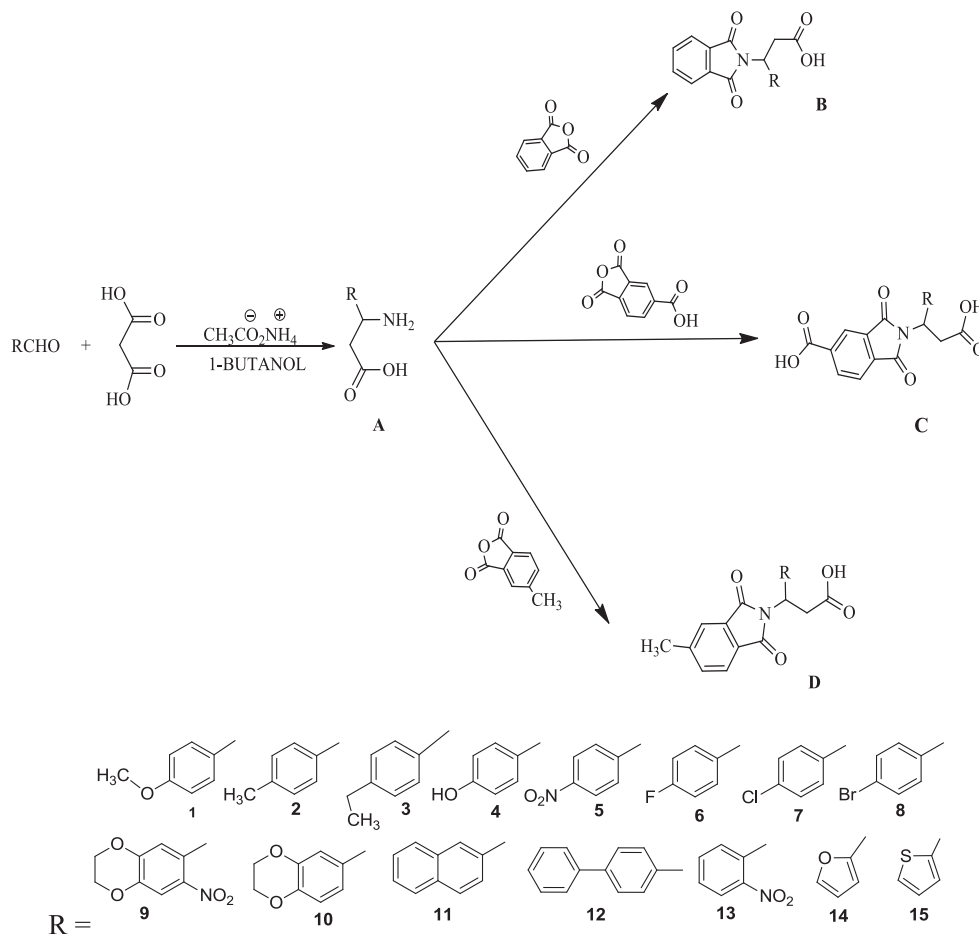


Fig. 6. 2D interaction of series D, B, C and A compounds with TcTS active residues, with highest to lowest TcTS inhibition percentage. The 2D image was produced by Discovery studio visualizer R-2 client 2017 version.

via hydrogen bonding with NO₂ substituents. Compound A-11 (Fig. 3 and 3-a) showed the highest predicted binding affinity (−9.0 kcal/mol) in this series. The hydrogen bond was found between Tyr342, Arg53 and Arg35 and a carboxylic oxygen atom, hydroxyl oxygen and the amino group of the 3-amino-3-arylpropionic acid chain. π - π stacking occurred between Val95 and the aromatic ring of naphthalene of compound A-11, but a hydrophobic interaction was found between Tyr119 and Trp312. The rest of the compounds A-9, A-10 and A-12, with the highest predicted binding affinity compared to the reference DANA, only showed interaction with two key amino acids, Arg245 and Glu230, but showed a hydrophobic interaction with other amino acids on the TcTS catalytic cavity. Therefore, from the docking analysis of series A, we concluded that the 3-amino-3-arylpropionic acid chain only has the ability to bind with two or three amino acid residues but no compound showed an interaction with Trp312 and other essential amino acid residues in the catalytic cavity of TcTS, even if they are small molecules that can be deep inside the catalytic cavity of TcTS.

In series B, the compound B-11 showed the highest binding affinity (−10.8 kcal/mol) (Table 1). The binding interaction of B-11 (Fig. 3 3-b) on TcTS cavity, showed that the arginine triad (Arg35, Arg245 and Arg314) was engaged by a carbonyl group of the phthaloyl moiety via hydrogen bonding. Also, Asp96 and Asp59 were attracted via π -anion interaction with naphthyl and phthaloyl groups of B-11 and Glu230 was found in interaction with the naphthyl group via π -anion. Additionally, hydrogen bonding between Glu230 and the −OH of the carboxylic acid group of B-11 was observed, while Tyr342 was bound via hydrogen bonding with the carbonyl group of phthaloyl. These results confirm the interaction of B-11 with three amino acid residues, Asp59, Glu230 and Tyr342, which is reported as very important to stabilize the transition state during the catalytic mechanism of sialic acid transfer of TcTS [38]. Moreover, Trp312, which contributes to the formation of the hydrophobic pocket and facilitates sialic acid transfer over hydrolysis and the formation of acceptor binding sites [10], was found in interaction with the phthaloyl ring of B-11 via the strongest



Scheme 1. Synthesized compounds and reaction conditions. Series A obtained by reflux for 2–3 h; Series B, C and D by fused reaction in the equimolar ratio at 250 °C.

Table 1
Predicted binding affinities of series A–D and natural ligand DANA on active site of TcTS using Auto Dock Vina version 4.2 and MGL.

Series A	*PBA	Series B	*PBA	Series C	*PBA	Series D	*PBA
A-1	−7.4	B-1	−9.1	C-1	−9.9	D-1	−9.6
A-2	−7.5	B-2	−9.9	C-2	−9.9	D-2	−9.7
A-3	−7.8	B-3	−9.4	C-3	−10.1	D-3	−10.0
A-4	−7.2	B-4	−9.3	C-4	−9.9	D-4	−9.6
A-5	−7.8	B-5	−9.5	C-5	−9.6	D-5	−9.6
A-6	−7.2	B-6	−9.2	C-6	−9.8	D-6	−9.0
A-7	−7.4	B-7	−9.3	C-7	−9.8	D-7	−9.6
A-8	−7.5	B-8	−9.2	C-8	−9.8	D-8	−9.7
A-9	−8.1	B-9	−9.8	C-9	−10.4	D-9	−10.5
A-10	−8.2	B-10	−9.4	C-10	−10.6	D-10	−10.5
A-11	−9.0	B-11	−10.8	C-11	−11.1	D-11	−11.1
A-12	−8.2	B-12	−9.0	C-12	−9.5	D-12	−9.4
A-13	−7.5	B-13	−9.2	C-13	−9.6	D-13	−9.6
A-14	−6.2	B-14	−8.0	C-14	−9.2	D-14	−8.8
A-15	−6.0	B-15	−7.0	C-15	−8.0	D-15	−8.2
DANA	−7.8	DANA	−7.8	DANA	−7.8	DANA	−7.8

*PBA= Predictive binding affinity in -Kcal/mol.

classical parallel π - π stacking. Furthermore, other residues, Tyr119, Trp120, Val95 and Leu176, which are involved in *trans* glycosylase activity and exclusion of water from the hydrophobic pocket [39,40] were attracted by B-11 with a hydrophobic interaction.

Compound B-2 showed the second highest predicted binding affinity (−9.9 kcal/mol) in this series, but the binding pattern was totally different compared to B-11. Only two key residues, Asp59 and Tyr342, which play an important role in protonation and

deprotonation of the TcTS enzyme in the transition state were bound via hydrogen bonding with the carbonyl group of the phthaloyl and the carbonyl group of carboxylic acid, respectively. The arginine triad only showed the weak Van der Waals forces. Val 95 and Asp96, two other important residues showed π -sigma and π -anion interaction with the phthaloyl ring.

Compounds B-6, B7 and B-8, which have halogen substituents showed the lowest predicted binding affinity compared to B-1, B-2 and B-3, which have electron donating substituents. Additionally, compounds B-5 and B-13 with a $-\text{NO}_2$ group at *para* and *meta* position of 3-arylpropionic acid, respectively, showed a large predicted binding affinity difference and binding pattern. The binding pattern of compound B-5 showed the three hydrogen bonding interactions, a $-\text{NO}_2$ group interaction with Trp312 and Arg245, a carboxylic group interaction with Tyr342 and a carbonyl group of phthaloyl interaction with Arg53 but in compound B-13 an unfavourable interaction of Glu230 was observed with carboxylic acid, while, a $-\text{NO}_2$ group showed hydrogen bonding with Tyr342 and Arg53, which is a totally different interaction compared to compound B-5.

Compounds B-14 and B-15 which contain furanyl and thienyl heterocyclic groups showed the same binding pattern as compound B-5 except the oxygen and sulphur atom showed an additional hydrogen bond with Tyr342 and Arg245. When the binding pattern of compound B-4 with a predicted binding affinity of −9.3 kcal/mol was compared with other compounds of this B series, only Trp120 showed a hydrogen bond between the oxygen atom of the hydroxyl group at the aryl moiety of propionic acid and all other residues

showed only hydrophobic interaction.

The compound B-12, with a bi-phenyl ring, showed the lowest predicted binding affinity values (-9.0 kcal/mol) compared to B-11, even though both have two aromatic rings, because the orientation pattern of B-12 in the catalytic cavity of the enzyme was found different compared to other compounds. The biphenyl ring did not show a strong interaction like the naphthalene ring of compound B-11. Only hydrogen binding was found between the carboxylic group and Tyr119.

The docking study of series C and D (Table 1), showed the same binding pattern and orientation in the catalytic pocket of TcTS as that of the B series with some exception due to the presence of carboxyl and methyl substituents at 4-position on the phthaloyl ring. One of the highest ranked compounds, C-11 with a predicted binding affinity of -11.1 kcal/mol (Fig. 3 and 3-c), showed an extra interaction due to the presence of a carboxylic acid group at 4-position on the phthaloyl ring bound to two extra amino acid residues, Tyr364 and Glu362, that were not reported as essential amino acids in the TcTS catalytic process but which are present in the catalytic pocket. Moreover, Glu230 of compound C-11 showed the π -anion interaction with the naphthyl ring; however, Glu230 was bound by hydrogen with an $-O$ atom of the hydroxyl group of the carboxylic group of propionic acid of compound B-11.

Compound D-11 (Fig. 3 and 3-d) with the highest predicted binding affinity (-11.1 kcal/mol) (Table 1) possessing a methyl group at 4-position on the phthaloyl ring showed the exact same binding pattern as that of compound C-11; only one more π -alkyl interaction was observed on the methyl group of the phthaloyl moiety with Trp312. In the case of the compound D-4 with a hydroxyl substituent on the aryl moiety of propionic acid, a hydrogen bond was found between the H atom of hydroxyl and the O atom of Asp96; also, the O atom of the hydroxyl group showed hydrogen bonding with Arg53. In a comparison of compound D-4 with C-4, the same binding pattern was observed in the $-OH$ group at *para* position of the aryl moiety of the propionic acid chain, but the oxygen atom of the carboxyl group of the propionic acid compound C-4 showed hydrogen bonding with Tyr119 and Arg245, while the same carboxyl group oxygen in D-4 showed hydrogen bonding with Glu230. A hydrophobic interaction was observed for Tyr119 and Arg245 for compound D-4. In addition, all the remaining compounds of series C and D showed the same binding pattern as was discussed for series B.

2.3. Enzyme inhibition

After molecular docking, twelve compounds from series A, B, C and D were selected according to the highest, intermediate and lowest predicted binding affinity to determine their inhibitory properties towards TcTS and to measure their capacity to inhibit the sialylation of *N*-acetylglucosamine in the reaction showed in Fig. 4. A mixture of 3'-sialyllactose (1 mM) donor, *N*-acetylglucosamine (1 mM) acceptor, and TcTS was prepared in the absence or presence of the inhibitor (1 mM) and analyzed by high-performance anion exchange chromatography with pulsed amperometric detection (HPAEC-PAD) [39,40].

Enzyme inhibition was calculated comparing the amount of 3'-sialyl-*N*-acetylglucosamine in the presence or absence of selected compounds. When the equimolar concentration of the donor substrate 3'-sialyllactose and inhibitors were used, inhibition values ranged between 1.4 and 86.9% (Fig. 5). Compounds D-11 and D-4 exhibited the strongest inhibition against TcTS with 86.9 and 82.5%, respectively. Furthermore, the compound B-14, C-11, B-11 and C-4 showed 76.5, 66.9, 65.8 and 53% enzyme inhibition, respectively. All compounds from series A showed lower inhibition values.

Interestingly, the compound D-11 with the highest inhibition

value, 86.9%, also showed the highest predicted binding affinity -11.1 kcal/mol compared to the reference DANA (-7.8 kcal/mol). However, compound C-11, which also has the same PBA value, exhibited a lower inhibition (66.9%). Both compounds, D-11 and C-11, bear the same substituents on the aryl group of the propionic acid part but different substituents, $-CH_3$ and $-COOH$ at 4-position, on the phthaloyl ring, respectively. On the other hand, compound B-11 with the same substituent on the aryl group, like compound D-11 and C-11, but with no substituents on the phthaloyl group, showed 65.8% enzyme inhibition, which is only one percent less than compound C-11. These results suggest that the addition of lipophilic or electron donating substituents on the phthaloyl moiety favour enzyme inhibition and TcTS inhibition values can be increased by the addition of these types of substituents.

2.3.1. Correlation between molecular docking and enzyme inhibition

Compound D-11 with 86.9% inhibition showed an interaction with the most essential amino acids on the active site of TcTS (Fig. 6) as follows: The carbonyl moiety of the phthaloyl group was found binding with two arginines (Arg35 and Arg314) and Tyr342 via a hydrogen bond. A classical π - π stacking was observed between Trp312 and phthaloyl ring, while methyl group at phthaloyl showed π -alkyl interaction. The naphthyl moiety at propionic acid and the phthaloyl group showed π - π stacking and π -anion interaction with Val95, Asp59 and Asp96, respectively. The amino acid Glu230 was found in hydrogen bonding with a proton of the hydroxyl group of the carboxylic acid of the propionic acid part and amino acid residues Tyr119, Trp120 and Arg245 were found in interaction via Van der Waals forces. The molecular docking analysis of compound C-11 and B-11 with 66.9 and 65.8% respectively, also showed the same pattern of interaction as shown by compound D-11, except the interaction of Glu230, which was found absent in compound C-11 (Fig. 6); however, an additional hydrogen bond interaction of Arg245 and Tyr119 was observed in compound C-11 which was absent in compound D-11.

Compound D-4 (Fig. 6), with the second highest inhibition value of 82.5%, in the docking analysis showed the same binding interaction for Arg35, Arg314, Asp59, Trp312, Glu230 and Tyr342 as compound D-11, except for the amino acid residues Asp96 and Arg53 which showed a hydrogen bond interaction with the *para* substituted hydroxyl group on the phenyl ring, at the propionic acid part of compound D-4.

On the other hand, compound C-4 which has the same scaffold as D-4, except for the $-COOH$ substituent at 4-position on the phthaloyl ring, showed 53% inhibition. The binding pattern of both compound C-4 and D-4 is about the same, except Glu230, which was found in a hydrogen bond interaction with a carboxylic group of a propionic acid part in D-4, but in compound C-4, Glu230 was found in π -anion interaction with the phenyl ring. Compound B-4 with the same scaffold-like compounds C-4 and D-4, but with no substituents on the phthaloyl moiety, showed only 5.6% inhibition. The interaction pattern of compound B-4 only showed a hydrophobic interaction with key amino acid residues in the TcTS catalytic pocket compared to the interaction pattern of compounds C-4 and D-11.

The compound B-14 with a furanyl ring showed the third highest TcTS enzyme inhibition, 76.5% (Fig. 6), compared to compounds C-14 and D-14, which have 40% and 19.2%, respectively. The interaction pattern of compound B-14 was found similar to compounds D-11 and D-4. Herein, Trp312 showed π - π stacking with the furanyl ring and hydrogen bonding with the carbonyl of the phthaloyl moiety. Furthermore, Tyr119 also showed π - π stacking and hydrogen bonding with the phthaloyl moiety but in compound D-11, D-4 and C-11, Tyr 119 was found in hydrophobic interaction.

In series A, compound A-11, which also has the highest predicted binding affinity (-9.0 kcal/mol) compared to DANA, showed the lowest enzyme inhibition value (8.3%). If we compare the interaction of A-11 with compounds that have the highest enzyme inhibition values (Fig. 6), we find that A-11 showed the lowest interaction with essential amino acids residues and also showed unfavourable interaction bumps, compared to other compound interactions with the highest predicted binding affinity and enzyme inhibition values.

From this correlation between molecular docking and enzymatic inhibition, we suggest that compounds with a strong interaction with Glu230, Trp312 and Tyr342 show a strong inhibition compared to other interactions and that the presence of lipophilic substituents ($-\text{CH}_3$) at 4-position on the phthaloyl moiety is another key factor to enhance inhibitory effects.

2.4. Trypanocidal activity

All synthesized compounds from series A, B, C and D were screened at a concentration of $10 \mu\text{g/mL}$ to determine their trypanocidal effect (% lysis) on a blood sample infected with trypomastigotes from NINOA and INC-5 strains of *T. cruzi*. Afterwards, compounds with a % lysis >50 were selected to determine the lysis concentration of 50% of the population (LC_{50}). Furthermore, C log P values, Absorption, Distribution, Metabolism, and Excretion (ADME) properties, pharmacokinetic properties of gastrointestinal absorption (GI) and blood-brain barrier (BBB) were predicted by using the online swissADME database (www.swissadme.com), and (www.cbligand.org/BBB/) respectively (Full results are shown in supporting material section).

2.4.1. 3-Amino-3-arylpropionic acid derivative series A

We began our investigation using 3-amino-3-arylpropionic acid derivative series A. The modification of substituents on the aryl moiety showed a different lytic effect on both NINOA and INC-5 strains. In series A, compounds A-1, A-2 and A-3 with electron donating substituents such as $-\text{OCH}_3$, $-\text{CH}_3$ and $-\text{C}_2\text{H}_5$ at *para*

position on the phenyl ring showed 83, 78 and 65% lysis, respectively, for NINOA strain (Table 2), values that are higher than that of the reference drugs Bzn (46.30%) and Nfx (40.74%). This showed that the alkyl substituent (methoxy) with an electronegative oxygen atom increases lysis. This may be due to more polarizability compared to the methyl substituent, but a comparison of the methyl and ethyl substituents showed that an increase in chain length decreases lysis. The electron withdrawing substituents $-\text{OH}$ and $-\text{NO}_2$ in compounds A-4 and A-5, respectively, at *para* position on the phenyl ring showed 50% lysis. When a substitution was made with naphthyl (A-11) and bi-phenyl (A-12) groups, only compound A-11 showed 60% lysis, which is better than the reference drugs, but compound A-12 showed a lower percentage of lysis (32%), which indicates that aromatic polarizability and conformers also have an important impact on lysis.

The compounds A-1 to A-3 with electron donating substituents, showed the lowest percentage of lysis, 54, 59 and 50%, respectively, for the INC-5 strain. This was about equal to the reference drugs Bzn 50% and Nfx 56% and less than the % lysis of these compounds for NINOA strain. This contrast in results may be due to different protein expression levels in trypomastigotes of both strains. In INC-5 strains, the compounds A-4 and A-5 with the electron withdrawing substituents $-\text{OH}$ and $-\text{NO}_2$, showed 76 and 68% lysis, respectively. This is better than the lysis of these compounds for NINOA strain. These lysis results indicate that electron withdrawing substituents favour lysis in INC-5. The compounds A-6 and A-7 with halogen atoms, such as $-\text{F}$ and $-\text{Cl}$, also showed good lysis, 62 and 73%, respectively.

Interestingly, compound A-11 with a naphthyl group showed 60% lysis which is exactly the same as with the NINOA strain. This suggests that the fused aromatic ring or the bulky aromatic moiety is favourable for both strains.

2.4.2. Phthaloyl derivatives of 3-amino-3-arylpropionic acids (series B)

In series B, the modification was made on the $-\text{NH}_2$ group of the 3-amino-3-arylpropionic acid series A derivatives by introducing a

Table 2

%Age lysis of trypomastigotes of NINOA and INC-5 strains, LC_{50} and C log P values of representative compounds of series A, B, C and D.

Compound	C log P	<i>T. cruzi</i> NINOA		<i>T. cruzi</i> INC-5	
		% Lysis at $10 \mu\text{g/mL}$	LC_{50} (μM)	% Lysis at $10 \mu\text{g/mL}$	LC_{50} (μM)
A-1	0.59	83 ± 6	101.53 ± 1.15	54 ± 2	256.12 ± 2.22
A-2	0.92	78 ± 4	183.68 ± 2.81	59 ± 3	290.14 ± 3.10
A-3	1.20	65 ± 3	113.09 ± 1.58	50 ± 7	263.90 ± 1.68
A-4	0.15	50 ± 4	151.52 ± 2.35	76 ± 2	127.38 ± 2.53
A-11	1.38	60 ± 6	98.66 ± 2.78	60 ± 3	102.88 ± 3.542
B-4	1.61	77 ± 4	71.38 ± 2.88	68 ± 1	90.96 ± 2.10
B-5	1.32	62 ± 5	53.49 ± 2.98	80 ± 1	118.63 ± 3.86
B-6	2.34	63 ± 2	90.81 ± 2.99	52 ± 3	81.41 ± 2.56
B-11	2.96	57 ± 2	97.27 ± 1.62	62 ± 4	117.26 ± 5.32
B-13	1.26	56 ± 6	Nd	68 ± 5	Nd
C-1	1.59	72 ± 4	Nd	32 ± 3	Nd
C-2	1.91	85 ± 5	109.50 ± 1.62	55 ± 2	39.88 ± 3.25
C-11	1.91	42 ± 4	Nd	24 ± 4	Nd
C-14	0.91	77 ± 6	77.57 ± 2.85	55 ± 3	101.61 ± 2.01
C-15	1.57	67 ± 5	Nd	19 ± 2	Nd
D-1	2.36	78 ± 7	65.57 ± 3.7	57 ± 4	59.46 ± 3.9
D-2	2.69	73 ± 8	85.57 ± 2.8	67 ± 6	43.57 ± 2.9
D-3	3.01	65 ± 4	Nd	59 ± 5	Nd
D-6	2.99	63 ± 6	45.18 ± 4.0	56 ± 6	74.63 ± 6.5
D-7	2.77	52 ± 6	37.70 ± 3.9	51 ± 7	52.01 ± 2.6
D-8	3.08	65 ± 6	24.59 ± 4.3	50 ± 6	23.02 ± 3.9
D-11	3.34	63 ± 4	52.70 ± 2.71	65 ± 2	46.19 ± 2.36
Bzn		46.30 ± 13.12	129.65 ± 5.1	56 ± 7	123.68 ± 4.51
Nfx		40.74 ± 6.4	89.52 ± 4.6	50 ± 6	77.23 ± 2.11

Nd = not determined.

phthaloyl group. This results in an increase of the C log P value (Table 2). The compounds B-4, B-5, B-13 and B-6 with –OH, –NO₂ (*meta* position for B-13), and –F at *para* position on the phenyl ring showed 77, 62, 63 and 56% lysis, respectively, for the NINOA strain (Table 2). This was greater than the reference drugs Bzn (46%) and Nfx (40%) and also better than compounds A-4, A-5, A-6 and A-13 for NINOA strain. The compound B-11 with a naphthyl group showed 60% lysis for NINOA strain. This is similar to compound A-11 in series A, which showed that the naphthyl moiety is unaffected by this phthaloyl addition.

Addition of a phthaloyl group produced the same effect on the INC-5 strain in series B as discussed above. A hydrophilic group (electron withdrawing), B-4, B-5, B-13 and B-7 with –OH, –NO₂ (*meta* position for B-13) and –Cl, at *para* position showed 68, 80, 70 and 68% lysis, respectively, but the activity of B-6 with an –F group decreased, and B-7 with a –Cl group increased compared to NINOA. This could be due to a biological difference in the strains. In a comparison of series A, the compounds A-4 to A-7 and A-13 showed about the same behaviour for the INC-5 strain. The compound B-11 with a naphthyl group showed a nearly similar 62% lysis, compared to the lysis for NINOA strain of compound A-11 as shown in series A. The rest of the compounds did not show better lysis than the reference drugs.

2.4.3. Carboxylic phthaloyl derivatives (series C)

In series C, a –COOH group was added at 4-position on the phthaloyl ring of series B. This addition caused a decrease in C log P values for all compounds compared to series B (Table 2). The compound C-2, with a –CH₃ substituent at *para* position on the phenyl ring showed the highest lysis, 85% for NINOA strain (Table 2). This was greater than all the compounds in series C and B. The compound C-1, with a methoxy substituent at the aryl ring showed the second highest lysis value, 72%, which was found to be about the same as compound C-1 but greater than compound B-1. This result showed that the addition of –COOH group at 4-position on the phthaloyl ring produced a better effect on lipophilic substituents on the aryl ring. Compound C-11 and C-12, with a naphthyl and a biphenyl ring at the aryl part of propionic acid, showed 42 and 17% lysis. This is less compared to compound B-11 and B-12, which showed that the addition of an electron withdrawing group at the phthaloyl moiety decreases lysis due to a decrease in electron density. The addition of a –COOH group at the phthaloyl moiety produced an appreciable effect on the lysis values of compounds C-14 and C-15 with heterocyclic moieties, such as furanyl and thienyl at the aryl part of propionic acid. These compounds showed 77 and 67% lysis, respectively, which is much better than the B-14 and B-15 compounds.

For INC-5 strain, compounds C-4, C-5 and C-13 with –OH and –NO₂ substituents at *para* and *meta* for C-13 showed 71, 63 and 68% lysis for INC-5 strain, which is greater compared to lysis of these compounds for NINOA strain but in comparison with the series B compounds, B-4, B-5 and B-13, compound C-4 showed a lower lysis and compound C-5 higher lysis. Compounds C-6 to C-8 with halogen substituents such as –F, –Cl, and –Br, respectively, showed 63, 67 and 69% lysis, respectively, which is better than the lysis of these compounds for NINOA and also better than series B compounds B-6 to B-8. Compound C-11 with a naphthyl group at the aryl part of propionic acid showed 24% lysis which was less than compound B-11 for INC-5 strain but an increase in lysis for compound C-13 was observed for INC-5 strain compared to lysis of the same compound for NINOA strain and B-12.

2.4.4. Methyl phthaloyl derivatives (series D)

In series D, the –CH₃ group was added at 4-position on the phthaloyl moiety, which showed an increase in C log P values for all

compounds compared to series B and C (Table 2). The compound D-1, D-2 and D-3 with a lipophilic substituent –OCH₃, –CH₃ and –C₂H₅ at *para* position on the phenyl ring of propionic acid showed 78, 73 and 65% lysis, respectively, for NINOA strain compared to the reference drugs Bzn (46%) and Nfx (40%) (Table 2). Compounds D-1–D-3 showed better % lysis compared to compounds B-1–B-3. In comparison with the series C compounds, C-1 and C-2, the series D compounds showed slightly better or equal lysis, but D-3 showed a higher lysis compared to a C-3 compound; this showed that the introduction of a lipophilic substituent on the phthaloyl group enhances the trypanocidal effect for ethyl group at the phenyl ring of the propionic acid part. Compounds D-6 to D-8 with halogen substituents (hydrophilic) –F, –Cl, and –Br at the *para* position on the phenyl ring showed 63, 62 and 65% lysis, respectively, for NINOA strain which is higher than compounds C-6 to C-8. In a comparison of compound D-6, compound B-6 showed a similar lysis but compound D-7 and D-8 showed a higher lysis than B-7 and B-8. These result of series D showed that the –CH₃ substituent at 4-position on the phthaloyl moiety increases the lysis of halogenated substituents. The –CH₃ (electron donating) on the phthaloyl moiety produced a good effect on the lytic activity of compound D-11 which has a naphthyl group, showing 63% lysis in NINOA compared to C-11 compound which has a –COOH group at 4-position on the phthaloyl ring and showed lysis similar to the B-11 compound of series B.

For INC-5 strain, compounds D-1 to D-3 with the lipophilic substituents OCH₃, –CH₃ and –C₂H₅ at *para* position on the phenyl ring of the propionic acid part, showed 57, 67 and 59% lysis activity which is better than compounds B-1 to B-3, and approximately similar to compounds C-1 to C-3 and the reference drugs Bzn (56%) and Nfx (50%) (Table 2). This finding indicates that the substituent on the phthaloyl moiety can enhance the lytic effect for INC-5 strain, compared to series B but no significant difference in lytic activity was observed for the –COOH and –CH₃ substituent on the phthaloyl moiety. Compound D-11 with a naphthyl group showed 65% lysis which is greater than a C-11 compound in series C and similar to compound B-11. This provides evidence that the addition of a more lipophilic substituent on the phthaloyl moiety can increase the lytic effect in INC-5 strain. A decrease in lysis of compound D-12, with a bi-phenyl substituent, was observed compared to C-12. The remaining compounds showed consistent behaviour as they have shown in series B and C for INC-5.

The different lytic effects of compounds in both NINOA and INC-5 strains showed that there are different protein expression and biochemical pathways [42] with different mechanisms of action for each compound in each series except in compounds with a naphthyl group in series A, B and D, which have shown the same consistency in results for both strains.

2.4.5. LC₅₀ determination

The LC₅₀ was determined only in the compounds with a percentage lysis >50 in both strains and whose value was lower than those of the reference drugs Bzn and Nfx, which showed LC₅₀ values (LC₅₀ = 129.56 ± 5.1 μM for NINOA and 102 ± 3.54 for INC-5 μM) and (LC₅₀ = 89.52 ± 4.6 μM for NINOA and 77.23 ± 2.11 μM for INC-5), respectively.

From series A, seven compounds A-1, A-2, A-3, A-4, A-5, A-11 and A-14 were selected for LC₅₀ determination (See supporting material section). From these compounds, A-11 showed the best biological activity with LC₅₀ values (98.66 ± 2.78 μM and 102.88 ± 3.542) similar in NINOA and INC-5 strains, respectively and better than reference drug Bzn.

From series B, compound B-4, B-5, B-6 and B-11 were selected to determine LC₅₀. All these compounds showed better LC₅₀ values on both strains compared to reference drug Bzn, but less than the Nfx

(Table 2). Most prominent LC₅₀ was showed by compound B-5 (LC₅₀ = 53.49 ± 2.98 μM) for NINOA strain.

From series C, compound C-2 showed the best trypanocidal activity on INC-5 strain (LC₅₀ = 39.88 ± 3.25 μM), compared to the reference drugs, but on NINOA this compound showed a low trypanocidal activity (LC₅₀ = 109.50 ± 1.62 μM). Compound C-14 showed LC₅₀ = 77.57 ± 2.85 μM for NINOA strain, which is better than the reference drugs, but on the INC-5 strain, the value was found greater than the reference drugs (LC₅₀ = 101.61 ± 2.01 μM) (Table 2).

In series D, six compounds D-1, D-2, D-6, D-7, D-8 and D-11 were selected to determine the LC₅₀ values (Table 2). Compound D-8 showed the most potent LC₅₀ for both strains, NINOA and INC-5 (LC₅₀ = 24.59 ± 4.3 and 23.02 ± 3.9 μM, respectively), while compound D-11 which also have the highest TcTS inhibition, showed LC₅₀ = 52.70 ± 2.1 μM for NINOA and 46.19 ± 2.3 μM for INC-5, which is better than the references.

3. Conclusions

In summary, fifteen 3-amino-3-aryl propionic acid derivatives (series A) and forty-five novel phthaloyl derivatives of 3-amino-3-aryl propionic acid (series B, C and D) were designed and synthesized with an excellent yield of 80–90%. The molecular docking analysis of these compounds on the TcTS enzyme revealed that compound C-11 (series C) and D-11 (series D) showed the highest predicted binding affinity –11.1 kcal/mol by hydrogen bonding, π–π stacking and Van der Waals forces with key amino acid residues Tyr342, Trp312, Arg53 and Glu230. HPAEC-PAD was used to determine the inhibition of selected compounds for the TcTS enzyme and found the following trend of inhibition D > B > C > A. Compounds D-11 and D-4 showed the highest predicted binding affinities 86.9% and 82.6%, respectively. This trend suggests that the high C log P and lipophilic substituents (-CH₃) on the phthaloyl moiety are important to increase TcTS inhibition. An *in vitro* test showed no correlation in trypanocidal activity between NINOA and INC-5 strain, due to the possibility of different protein expression, but series D compounds showed better lysis activity and LC₅₀ for both strains. Series A (3-amino-3-arylpropionic acid) also showed good LC₅₀ values but poor enzyme inhibition, which suggests that these compounds have another mechanism of action.

A strong correlation between molecular docking and enzyme inhibition was found for compound D-11 (86.9% inhibition and –11.1 kcal/mol binding affinity) with good trypanocidal activity for both strains. ADME prediction showed that these compounds have high gastrointestinal absorption (GI) values; some even have positive BBB (blood brain barrier) values and follow Lipinski properties for drug development. Therefore, these phthaloyl derivatives could be used as TcTS inhibitors to develop new anti-Chagas drugs.

4. Experimental

4.1. Chemistry

All reactive, solvents were purchased from Sigma-Aldrich and were used without further purification. Melting points were determined on Mel-Temp capillary apparatus and are uncorrected. The solvent evaporation under vacuum was carried out by using BUCHI Rotavapor® R-100. The purity and reactions were monitored by thin-layer chromatography (TLC) performed on silica gel plates prepared with silica gel 60 (PF-245 with gypsum, Merck Japan), of the thickness of 0.25 mm. The developed chromatograms were visualized under ultraviolet light at 254–265 nm. Infrared spectra were recorded using OPUS_7.5.18 software with PLATINUM-ATR

Bruker Alpha FT-IR spectrometer. NMR data were collected with Bruker Avance 500 spectrometer operating at 500 MHz (¹H), and 126 MHz (¹³C). ¹H proton NMR spectra were obtained in DMSO-*d*₆, with TMS as an internal standard. Chemical shifts are given on the δ scale (ppm). Multiplicities are indicated as follows: s (singlet), d (doublet), t (triplet), q (quartet), m (multiplet) or br (broadened).

4.1.1. General procedure for preparation series A compounds A-1 to A-15

A mixture of appropriate aldehyde 2.40 g (1–15), 2.44 g of malonic acid and 3.54 g of ammonium acetate (1:1.1:2.3), in 200 mL of the 1-butanol was refluxed for 1.5–2 h until the evolution of CO₂ ceased. The precipitate formed was filtered and washed with boiling 1-butanol (2 × 50 mL), boiling ethanol (2 × 50 mL) and 100 mL of water. Precipitates were dried at 80–100 °C for 8–10 h. Purity of product was checked by TLC, and yield obtained about 65–80% in each reaction.

4.1.1.1. 3-Amino-3-(4-methoxyphenyl)propanoic acid (A-1). Yield: 70%, mp 236–8 °C, FT IR (cm⁻¹): 3250–2900 (NH₃⁺), 3050 (CH sp²), 1613_{asym} (C=O), 1255 (C-O), 1156 (C-N). ¹H NMR (500 MHz, DMSO-*d*₆): δ 7.11 (d, 2H, C₆H₄), 6.77 (d, 2H, C₆H₄), 4.12 (q, 1H, CHN), 3.61 (s, 3H, OCH₃), 2.32–2.41 (d, 2H, CHCH₂). ¹³C NMR (126 MHz, DMSO-*d*₆): δ 179.3, 161.8, 137.5, 129.7, 118.4, 59.8, 53.3, 49.1.

4.1.1.2. 3-Amino-3-(*p*-tolyl)propanoic acid (A-2). Yield: 67%, mp 223–5 °C, FT IR (ν cm⁻¹): 3200–2970 (NH₃⁺), 3070 (CH sp²), 1619_{asym} (C=O), 1268 (C-O), 1145 (C-N). ¹H NMR (500 MHz, DMSO-*d*₆): δ 7.21–7.30 (m, 2H, C₆H₄), 6.90–6.77 (m, 2H, C₆H₄), 4.31 (q, 1H, CHN), 2.27–2.39 (d, 2H, CHCH₂), 2.11 (s, 3H, CH₃). ¹³C NMR (126 MHz, DMSO-*d*₆): δ 170.9, 139.4134.8, 128.1, 126.0, 119.9, 51.0, 39.2, 18.9.

4.1.1.3. 3-Amino-3-(4-ethylphenyl)propanoic acid (A-3). Yield: 71%, mp 240–2 °C, FT IR (ν cm⁻¹): 3240–2885 (NH₃⁺), 3055 (CH sp²), 1647_{asym} (C=O), 1265 (C-O), 1162 (C-N). ¹H NMR (500 MHz, DMSO-*d*₆): δ 7.20–7.31 (m, 2H, C₆H₄), 6.90–6.79 (m, 2H, C₆H₄), 4.38 (q, 1H, CHN), 2.32–2.30 (d, 2H, CHCH₂), 2.11 (q, 2H, CH₂CH₃), 1.39 (t, 3H, CH₂CH₃); ¹³C NMR (126 MHz, DMSO-*d*₆): δ 178.3, 143.4, 141.3, 131.5, 127.8, 127.7, 126.3126.0, 50.1, 33.4, 19.1.

4.1.1.4. 3-Amino-3-(4-hydroxyphenyl)propanoic acid (A-4). Yield: 70%, mp 194–6 °C, FT IR (ν cm⁻¹): 3190–2910 (NH₃⁺), 2999 (CH sp²), 1620_{asym} (C=O), 1258 (C-O), 1147 (C-N). ¹H NMR (500 MHz, DMSO-*d*₆): δ 7.16–7.20 (m, 2H, C₆H₄), 6.74–6.80 (m, 2H, C₆H₄), 4.60 (s, 1H, C₆H₄OH), 4.39 (q, 1H, CHN), 2.49–2.38 (d, 2H, CHCH₂). ¹³C NMR (126 MHz, DMSO-*d*₆): δ 171.2, 142.3, 134.5, 130.8, 123.6, 51.1, 38.2.

4.1.1.5. 3-Amino-3-(4-nitrophenyl)propanoic acid (A-5). Yield: 69%, mp 211–3 °C, FT IR (ν cm⁻¹): 3210–2990 (NH₃⁺), 3020 (CH sp²), 1637_{asym} (C=O), 1557 (NO₂), 1275 (C-O), 1173 (C-N). ¹H NMR (500 MHz, DMSO-*d*₆): δ 7.19–7.23 (m, 2H, C₆H₄), 6.78–6.86 (m, 2H, C₆H₄), 4.41 (q, 1H, CHN), 3.32–2.21 (d, 2H, CHCH₂). ¹³C NMR (126 MHz, DMSO-*d*₆): δ 174.2, 151, 145.3, 132.5, 129.8, 121.6, 50.1, 37.1.

4.1.1.6. 3-Amino-3-(4-fluorophenyl)propanoic acid (A-6). Yield: 72%, mp 231–3 °C, FT IR (ν cm⁻¹): 3290–2916 (NH₃⁺), 3038 (CH sp²), 1620_{asym} (C=O), 1268 (C-O), 1163 (C-N), 832 (C-F). ¹H NMR (500 MHz, DMSO-*d*₆): δ 7.15–7.25 (m, 2H, C₆H₄), 7.01–7.11 (m, 2H, C₆H₄), 4.21 (q, 1H, CHN), 2.31–2.62 (d, 2H, CHCH₂); ¹³C NMR (126 MHz, DMSO-*d*₆): δ 172.9, 164.8, 131.5, 130.4, 117.7, 51.4, 38.8.

4.1.1.7. 3-Amino-3-(4-chlorophenyl)propanoic acid (A-7). Yield:

75%, mp 224–6 °C FT IR (ν cm⁻¹): 3270–2933 (NH₃⁺), 3010 (CH sp²), 1647_{asym} (C=O), 1269 (C-O), 1153 (C-N), 805 (C-Cl). ¹H NMR (500 MHz, DMSO-*d*₆): δ 7.29–7.30 (m, 2H, C₆H₄), 7.12–7.18 (m, 2H, C₆H₄), 4.52 (q, 1H, CHN), 2.61–2.72 (d, 2H, CHCH₂); ¹³C NMR (126 MHz, DMSO-*d*₆): δ 178.8, 142.9, 135.5, 131.4, 124.7, 51.4, 37.9.

4.1.1.8. 3-Amino-3-(4-bromophenyl)propanoic acid (A-8). Yield: 72%, mp 236–8 °C, FT IR (ν cm⁻¹): 3280–2875 (NH₃⁺), 3088 (CH sp²), 1645_{asym} (C=O), 1247 (C-O), 1177 (C-N), 710 (C-Br). ¹H NMR (500 MHz, DMSO-*d*₆): δ 7.25–7.37 (m, 2H, C₆H₄), 7.14–7.20 (m, 2H, C₆H₄), 4.10 (q, 1H, CHN), 2.35–2.43 (d, 2H, CHCH₂). ¹³C NMR (126 MHz, DMSO-*d*₆): 171.7, 140.1, 135.7, 132.7, 129.4, 124.1, 51.8, 37.9.

4.1.1.9. 3-Amino-3-(7-nitro-2,3-dihydrobenzo[b][1,4]dioxin-6-yl)propanoic acid (A-9). Yield: 70%, mp 225–7 °C FT IR (ν cm⁻¹): 3300–3100 (NH₃⁺), 2970 (CH sp²), 1649_{asym}, 1570 (NO₂), 1281 (C-O), 1179 (C-N). ¹H NMR (500 MHz, DMSO-*d*₆): δ 7.51 (s, 1H, C₆H₂), 7.28 (s, 1H, C₆H₂), 4.43 (s, 4H, C₂H₄O), 4.28 (q, 1H, CHN), 2.28–2.21 (d, 2H, CHCH₂). ¹³C NMR (126 MHz, DMSO-*d*₆): δ 175.1, 151.1, 141.9, 131.2, 130.7, 119.2, 65.1, 65.1, 50.0, 41.1.

4.1.1.10. 3-Amino-3-(2,3-dihydrobenzo[b][1,4]dioxin-6-yl)propanoic acid (A-10). Yield: 67%, mp 214–6 °C, FT IR (ν cm⁻¹): 3320–2980 (NH₃⁺), 2988 (CH sp²), 1629_{asym} (C=O), 1278 (C-O), 1136 (C-N). ¹H NMR (500 MHz, DMSO-*d*₆): δ 7.12 (s, 1H, C₆H₃), 6.91–6.82 (m, 2H, C₆H₃), 4.34 (m, 2H, C₂H₄O₂), 4.18 (q, 1H, CHN), 2.24–2.19 (d, 2H, m, 2H, CHCH₂). ¹³C NMR (126 MHz, DMSO-*d*₆): δ 173.8, 152.3, 143.1, 132.0, 130.9, 118.2, 64.8, 64.8, 49.1, 39.2.

4.1.1.11. 3-Amino-3-(naphthalen-2-yl)propanoic acid (A-11). Yield: 80%, mp 217–9 °C, FT IR (ν cm⁻¹): 3390–2965 (NH₃⁺), 3049 (CH sp²), 1632_{asym} (C=O), 1284 (C-O), 1155 (C-N). ¹H NMR (500 MHz, DMSO-*d*₆): δ 7.99–7.90 (m, 3H, C₁₂H₇), 7.58–7.47 (m, 3H, C₁₂H₇), 7.18 (t, 1H, C₁₂H₇), 4.51 (q, 1H, CHN), 2.37–2.30 (d, 2H, CHCH₂). ¹³C NMR (126 MHz, DMSO-*d*₆): δ 174.3, 139.7, 133.2, 133.1, 128.6, 128.5, 127.9, 123.1, 52.8, 42.7.

4.1.1.12. 3-([1,1'-biphenyl]-4-yl)-3-aminopropanoic acid (A-12). Yield: 74%, mp 237–9 °C, FT IR (ν cm⁻¹): 3380–2920 (NH₃⁺), 3022 (CH sp²), 1634_{asym} (C=O), 1247 (C-O), 1167 (C-N). ¹H NMR (500 MHz, DMSO-*d*₆): δ 7.17–7.48 (m, 9H, C₁₂H₉), 4.16 (q, 1H, CHN), 2.48–2.57 (m, 2H, CHCH₂). ¹³C NMR (126 MHz, DMSO-*d*₆): δ 174.2, 136.5, 136.4, 135.1, 128.3, 128.2, 128.1, 128.0, 127.9, 126.2, 126.0, 125.4, 52.2, 41.7.

4.1.1.13. 3-Amino-3-(2-nitrophenyl)propanoic acid (A-13). Yield: 75%, mp 212–4 °C FT IR (ν cm⁻¹): 3290–2965 (NH₃⁺), 3006 (CH sp²), 1629_{asym} (C=O), 1552 (NO₂), 1258 (C-O), 1166 (C-N). ¹H NMR (500 MHz, DMSO-*d*₆): δ 7.97–7.70 (m, 2H, C₆H₄), 7.64–7.57 (m, 2H, C₆H₄), 4.39 (q, 1H, CHN), 2.44–2.37 (d, 2H, CHCH₂). ¹³C NMR (126 MHz, DMSO-*d*₆): δ 173.9, 153, 144.1, 134.2, 130.1, 124.4, 51.7, 40.7.

4.1.1.14. 3-Amino-3-(furan-2-yl)propanoic acid (A-14). Yield: 70%, mp 186–9 °C FT IR (ν cm⁻¹): 3385–3020 (NH₃⁺), 3001 (CH sp²), 1635_{asym} (C=O), 1248 (C-O), 1157 (C-N). ¹H NMR (500 MHz, DMSO-*d*₆): δ 7.53 (d, 1H, C₄H₄O), 6.55 (t, 1H, C₄H₄O), 6.28 (d, 1H, C₄H₄O), 4.29 (q, 1H, CHN), 2.41–2.34 (d, 2H, CHCH₂). ¹³C NMR (126 MHz, DMSO-*d*₆): δ 171.2, 153.2, 141.4, 110.3, 101.1, 51.8, 37.8.

4.1.1.15. 3-Amino-3-(thiophen-2-yl)propanoic acid (A-15). Yield: 67%, mp 201–3 °C, FT IR (ν cm⁻¹): 3380–2999 (NH₃⁺), 2972 (CH sp²), 1620_{asym} (C=O), 1274 (C-O), 1162 (C-N), 692 (C-S). ¹H NMR (500 MHz, DMSO-*d*₆): δ 7.42 (d, 1H, C₄H₄S), 7.02 (s, 1H, C₄H₄S), 6.88

(d, 1H, C₄H₄S), 4.52 (q, 1H, CHN), 2.58–2.40 (d, 2H, CHCH₂). ¹³C NMR (126 MHz, DMSO-*d*₆): δ 173.2, 130.8, 129.2, 128.9, 128.1, 51.4, 42.6.

4.1.2. General procedure for the synthesis of phthaloyl derivatives of 3-amino-3-arylpropionic acids (series B, C, & D)

Compounds in three series (16–60) were synthesized by fused reaction. Equimolar (1:1) amount of appropriate 3-amino-3-arylpropionic acids and phthalic anhydride (series B), trimellitic anhydride (series C) and 4-methylphthalic anhydride (series D) were grinded to form homogenised mixture. The mixture was taken in 50 mL reaction flask and placed in oil bath at 250 °C, until the mixture fused. The reaction flask was kept at room temperature for 30 min and product was obtained. The product was recrystallized in methanol and washed with acetone and chloroform. Purity of product was checked by TLC, and yield obtained about 85–90% in each reaction.

4.1.2.1. 3-(1,3-Dioxoisindolin-2-yl)-3-(4-methoxyphenyl)propanoic acid (B-1). Yield: 85%, mp 109–1 °C FT IR (ν cm⁻¹): 3285–2901 (OH), 2988 (CH sp²), 1769_{asym}, 1699_{sym} (NC₂O₂), 1609_{asym}, 1354_{sym} (C=O), 1247 (C-O), 1176 (C-N). ¹H NMR (500 MHz, DMSO-*d*₆): δ 12.37 (s, 1H, COOH), 7.71 (m, 2H, C₆H₄), 7.63 (m, 2H, C₆H₄), 7.41–7.32 (m, 2H, C₆H₄), 6.89–6.87 (m, 2H, C₆H₄), 5.47 (br t, 1H, C₂O₂NH), 3.62 (s, C₆H₄OCH₃), 3.52–3.10 (d, 2H, NHCH₂). ¹³C NMR (126 MHz, DMSO-*d*₆): δ 172.3, 168.3, 168.3, 159.1, 135.3, 135.3, 132.3, 131.5, 131.5, 128.2, 123.5, 123.5, 114.3, 114.1, 55.4, 50.4, 40.1.

4.1.2.2. 3-(1,3-Dioxoisindolin-2-yl)-3-(*p*-tolyl)propanoic acid (B-2). Yield: 86%, mp 102–5 °C FT IR (ν cm⁻¹): 3310–2958 (OH), 3030 (CH sp²), 1770_{asym}, 1699_{sym} (NC₂O₂), 1610_{asym}, 1363_{sym} (C=O), 1215 (C-O), 1169 (C-N). ¹H NMR (500 MHz, DMSO-*d*₆): δ 12.49 (s, 1H, COOH), 7.85 (m, 2H, C₆H₄), 7.78 (m, 2H, C₆H₄), 7.30–7.14 (m, 2H, C₆H₄), 7.10–6.92 (m, 2H, C₆H₄), 5.65 (br t, 1H, C₂O₂NH), 3.51–3.29 (d, 2H, NHCH₂), 2.23 (s, 3H, C₆H₄CH₃). ¹³C NMR (126 MHz, DMSO-*d*₆): δ 172.7, 168.8, 168.8, 144.0, 141.2, 135.2, 134.9, 134.9, 132.3, 131.8, 131.4, 128.4, 123.6, 123.4, 114.2, 114.2, 50.4, 39.6, 22.1.

4.1.2.3. 3-(1,3-Dioxoisindolin-2-yl)-3-(4-ethylphenyl)propanoic acid (B-3). Yield: 87%, mp 116–9 °C, FT IR (ν cm⁻¹): 3288–2990 (OH), 3028 (CH sp²), 1770_{asym}, 1700_{sym} (NC₂O₂), 1611_{asym}, 1353_{sym} (C=O), 1215 (C-O), 1170 (C-N). ¹H NMR (500 MHz, DMSO-*d*₆): δ 12.38 (s, 1H, COOH), 7.81 (m, 2H, C₆H₄), 7.62 (m, 2H, C₆H₄), 7.48–7.37 (m, 2H, C₆H₄), 7.10–7.03 (m, 2H, C₆H₄), 5.43 (br t, 1H, C₂O₂NH), 3.43–3.34 (d, 2H, NHCH₂), 2.32 (q, 2H, C₆H₄CH₂CH₃), 1.51 (t, 3H, C₆H₄CH₂CH₃). ¹³C NMR (126 MHz, DMSO-*d*₆): δ 174.2, 168.1, 168.1, 145.2, 141.8, 135.7, 135.4, 129.2, 129.0, 127.9, 127.3, 125.1, 124.5, 52.1, 41.1, 28.2, 14.4.

4.1.2.4. 3-(1,3-Dioxoisindolin-2-yl)-3-(4-hydroxyphenyl)propanoic acid (B-4). Yield: 85%, mp 136–8 °C FT IR (ν cm⁻¹): 3392–2899 (OH), 3058 (CH sp²), 1772_{asym}, 1691_{sym} (NC₂O₂), 1608_{asym}, 1384_{sym} (C=O), 1267 (C-O), 1169 (C-N). ¹H NMR (500 MHz, DMSO-*d*₆): δ 12.43 (s, 1H, COOH), 7.70 (m, 2H, C₆H₄), 7.66 (m, 2H, C₆H₄), 7.20–7.15 (m, 2H, C₆H₄), 6.77–6.69 (m, 2H, C₆H₄), 5.77 (s, 1H, C₆H₄OH), 5.51 (br t, 1H, C₂O₂NH), 3.19–3.10 (d, 2H, NHCH₂). ¹³C NMR (126 MHz, DMSO-*d*₆): δ 173.8, 169.1, 169.1, 160.0, 141.8, 139.3, 136.4, 133.8, 132.0, 130.4, 129.4, 129.1, 119.7, 119.0, 52.1, 41.2.

4.1.2.5. 3-(1,3-Dioxoisindolin-2-yl)-3-(4-nitrophenyl)propanoic acid (B-5). Yield: 88%, mp 152–5 °C FT IR (ν cm⁻¹): 3378–2950 (OH), 3059 (CH sp²), 1773_{asym}, 1702_{sym} (NC₂O₂), 1630_{asym}, 1380_{sym} (C=O), 1545 (NO₂), 1280 (C-O), 1181 (C-N). ¹H NMR (500 MHz, DMSO-*d*₆): δ 12.54 (s, 1H, COOH), 8.11–8.14 (m, 2H, C₆H₄), 7.98 (m, 2H, C₆H₄), 7.88 (m, 2H, C₆H₄), 7.64–7.67 (m, 2H, C₆H₄), 5.41 (br t, 1H, C₂O₂NH), 3.39–3.24 (d, 2H, NHCH₂). ¹³C NMR (126 MHz, DMSO-*d*₆):

δ 171.8, 167.1, 167.1, 150.6, 147.8, 143.4, 137.0, 132.6, 131.7, 131.0, 130.5, 124.2, 123.8, 123.7, 123.4, 51.8, 41.1.

4.1.2.6. 3-(1,3-Dioxoisindolin-2-yl)-3-(4-fluorophenyl)propanoic acid (B-6). Yield: 80%, mp 162–4 °C FT IR (ν cm⁻¹): 3420–2910 (OH), 3058 (CH sp²), 1770_{asym}, 1702_{sym} (NC₂O₂), 1602_{asym}, 1383_{sym} (C=O), 1221 (C-O), 1160 (C-N), 823 (C-F). ¹H NMR (500 MHz, DMSO-d₆): δ 12.39 (s, 1H, COOH), 7.89–7.80 (m, 4H, C₆H₄), 7.31–7.21 (m, 4H, C₆H₄), 5.42 (br t, 1H, C₂O₂NH), 3.22–3.14 (d, 2H, NHCH₂). ¹³C NMR (126 MHz, DMSO-d₆): δ 172.9, 167.6, 167.6, 164.3, 148.1, 142.4, 136.6, 133.1, 130.4, 129.3, 129.1, 124.8, 124.5, 116.9, 116.7, 52.1, 39.6.

4.1.2.7. 3-(4-chlorophenyl)-3-(1,3-dioxoisindolin-2-yl)propanoic acid (B-7). Yield: 85%, mp 158–0 °C FT IR (ν cm⁻¹): 3402–2945 (OH), 3047 (CH sp²), 1771_{asym}, 1700_{sym} (NC₂O₂), 1626_{asym}, 1352_{sym} (C=O), 1225 (C-O), 1176 (C-N), 793 (C-Cl). ¹H NMR (500 MHz, DMSO-d₆): δ 12.47 (s, 1H, COOH), 7.72–7.67 (m, 4H, C₆H₄), 7.54–7.49 (m, 4H, C₆H₄), 5.39 (br t, 1H, C₂O₂NH), 3.11–2.99 (d, 2H, NHCH₂). ¹³C NMR (126 MHz, DMSO-d₆): δ 172.7, 167.9, 167.9, 146.1, 141.8, 141.5, 138.6, 136.4, 134.1, 134.0, 133.1, 132.4, 129.01, 128.1, 51.4, 40.7.

4.1.2.8. 3-(4-bromophenyl)-3-(1,3-dioxoisindolin-2-yl)propanoic acid (B-8). Yield: 85%, mp 162–4 °C FT IR (ν cm⁻¹): 3310–2975 (OH), 3050 (CH sp²), 1771_{asym}, 1700_{sym} (NC₂O₂), 1606_{asym}, 1385_{sym} (C=O), 1287 (C-O), 1173 (C-N), 713 (C-Br). ¹H NMR (500 MHz, DMSO-d₆): δ 12.33 (s, 1H, COOH), 7.96 (m, 2H, C₆H₄), 7.86–7.82 (m, 4H, C₆H₄), 7.28–7.22 (m, 2H, C₆H₄), 5.41 (br t, 1H, C₂O₂NH), 3.11–3.08 (d, 2H, NHCH₂). ¹³C NMR (126 MHz, DMSO-d₆): δ 173.1, 166.7, 166.5, 144.1, 135.8, 135.4, 135.1, 132.0, 131.8, 131.8, 130.4, 128.8, 127.6, 125.4, 124.2, 52.5, 41.2.

4.1.2.9. 3-(1,3-Dioxoisindolin-2-yl)-3-(7-nitro-2,3-dihydrobenzo[b][1,4]dioxin-6-yl)propanoic acid (B-9). Yield: 78%, mp 155–8 °C, FT IR (ν cm⁻¹): 3198–2950 (OH), 3064 (CH sp²), 1771_{asym}, 1706_{sym} (NC₂O₂), 1608_{asym}, 1390_{sym} (C=O), 1511 (NO₂), 1257 (C-O), 1159 (C-N). ¹H NMR (500 MHz, DMSO-d₆): δ 12.46 (s, 1H, COOH), 7.88–7.85 (m, 4H, C₆H₄), 7.19 (d, 1H, C₆H₄), 7.10 (d, 1H, C₆H₄), 5.47 (br t, 1H, C₂O₂NH), 4.08 (m, 4H, C₆H₃O₂C₂H₄), 3.11–3.02 (d, 2H, NHCH₂). ¹³C NMR (126 MHz, DMSO-d₆): δ 173.1, 167.3, 167.3, 152.1, 149.3, 144.1, 140.1, 140.4, 138.4, 132.1, 130.1, 129.1, 125.0, 123.1, 67.1, 67.1, 53.5, 42.1.

4.1.2.10. 3-(2,3-dihydrobenzo[b][1,4]dioxin-6-yl)-3-(1,3-dioxoisindolin-2-yl)propanoic acid (B-10). Yield: 85%, mp 165–8 °C, FT IR (ν cm⁻¹): 3423–2980 (OH), 3042 (CH sp²), 1766_{asym}, 1698_{sym} (NC₂O₂), 1611_{asym}, 1380_{sym} (C=O), 1250 (C-O), 1170 (C-N). ¹H NMR (500 MHz, DMSO-d₆): δ 12.39 (s, 1H, COOH), 7.78–7.74 (m, 4H, C₆H₄), 6.76–6.70 (m, 3H, C₆H₄), 5.41 (br t, 1H, C₂O₂NH), 4.17 (m, 4H, C₆H₃O₂C₂H₄), 3.11–2.99 (d, 2H, NHCH₂). ¹³C NMR (126 MHz, DMSO-d₆): δ 172.9, 167.1, 167.1, 146.3, 146.0, 143.1, 135.1, 134.4, 132.0, 131.3, 130.0, 123.2, 118.4, 117.0, 114.0, 66.2, 66.2, 52.1, 41.8.

4.1.2.11. 3-(1,3-Dioxoisindolin-2-yl)-3-(naphthalen-2-yl)propanoic acid (B-11). Yield: 83%, mp 131–4 °C. FT IR (ν cm⁻¹): 3205–2901 (OH), 3071 (CH sp²), 1771_{asym}, 1698_{sym} (NC₂O₂), 1624_{asym}, 1378_{sym} (C=O), 1286 (C-O), 1171 (C-N). ¹H NMR (500 MHz, DMSO-d₆): δ 12.01 (s, 1H, COOH), 8.10–7.88 (m, 3H, C₁₀H₇), 7.86–7.85 (m, 4H, C₆H₄), 7.63–7.61 (m, 2H, C₁₀H₇), 7.21 (d, 1H, C₁₀H₇), 5.63 (br t, 1H, C₂O₂NH), 3.44–3.38 (d, 2H, NHCH₂). ¹³C NMR (126 MHz, DMSO-d₆): δ 172.8, 167.3, 167.3, 145.8, 144.3, 136.9, 133.5, 133.3, 132.6, 132.4, 131.0, 130.8, 130.1, 129.8, 129.7, 129.6, 129.0, 128.7, 128.6, 53.1, 42.5.

4.1.2.12. 3-([1,1'-biphenyl]-4-yl)-3-(1,3-dioxoisindolin-2-yl)propanoic acid (B-12). Yield: 80%, mp 152–5 °C FT IR (ν cm⁻¹): 3415–2888 (OH), 3031 (CH sp²), 1772_{asym}, 1702_{sym} (NC₂O₂),

1627_{asym}, 1382_{sym} (C=O), 1287 (C-O), 1172 (C-N). ¹H NMR (500 MHz, DMSO-d₆): δ 12.44 (s, 1H, COOH), 7.85–7.83 (s, 4H, C₆H₄), 7.47–7.15 (m, 9H, C₁₂H₉), 5.70 (br t, 1H, C₂O₂NH), 3.40–3.30 (d, 2H, NHCH₂). ¹³C NMR (126 MHz, DMSO-d₆): δ 172.4, 168.1, 168.1, 151.7, 147.6, 133.0, 132.9, 132.8, 132.6, 131.0, 129.9, 129.8, 129.6, 129.5, 129.4, 129.2, 129.0, 128.1, 128.0, 55.1, 44.4.

4.1.2.13. 3-(1,3-Dioxoisindolin-2-yl)-3-(2-nitrophenyl)propanoic acid (B-13). Yield: 78%, mp 162–5 °C FT IR (ν cm⁻¹): 3400–2970 (OH), 3057 (CH sp²), 1772_{asym}, 1703_{sym} (NC₂O₂), 1630_{asym}, 1373_{sym} (C=O), 1571 (NO₂), 1289 (C-O), 1183 (C-N). ¹H NMR (500 MHz, DMSO-d₆): δ 12.62 (s, 1H, COOH), 8.15 (m, 1H, C₆H₄), 7.99–7.92 (m, 4H, C₆H₄), 7.71–7.68 (m, 3H, C₆H₄), 5.77 (br t, 1H, C₂O₂NH), 3.21–3.08 (d, 2H, NHCH₂). ¹³C NMR (126 MHz, DMSO-d₆): δ 173.1, 168.0, 168.0, 152.3, 147.8, 144.0, 138.0, 132.1, 131.2, 130.7, 130.4, 123.5, 123.4, 123.3, 123.2, 53.1, 42.1.

4.1.2.14. 3-(1,3-Dioxoisindolin-2-yl)-3-(furan-2-yl)propanoic acid (B-14). Yield: 85%, mp 175–8 °C, FT IR (ν cm⁻¹): 3410–2930 (OH), 3047 (CH sp²), 1772_{asym}, 1713_{sym} (NC₂O₂), 1604_{asym}, 1384_{sym} (C=O), 1286 (C-O), 1182 (C-N). ¹H NMR (500 MHz, DMSO-d₆): δ 11.99 (s, 1H, COOH), 7.86–7.45 (m, 4H, C₆H₄), 7.55 (m, 1H, C₄H₃O), 7.20–6.69 (m, 2H, C₄H₃O), 5.54 (br t, 1H, C₂O₂NH), 3.28–3.02 (d, 2H, NHCH₂). ¹³C NMR (126 MHz, DMSO-d₆): δ 172.2, 167.0, 167.0, 159.0, 145.4, 143.7, 141.7, 135.2, 133.8, 128.6, 123.1, 117.1, 116.3, 53.0, 43.1.

4.1.2.15. 3-(1,3-Dioxoisindolin-2-yl)-3-(thiophen-2-yl)propanoic acid (B-15). Yield: 83%, mp 169–1 °C, FT IR (ν cm⁻¹): 3400–2900 (OH), 3058 (CH sp²), 1771_{asym}, 1707_{sym} (NC₂O₂), 1619_{asym}, 1367_{sym} (C=O), 1281 (C-O), 1185 (C-N). ¹H NMR (500 MHz, DMSO-d₆): δ 11.55 (s, 1H, COOH), 7.77–7.40 (m, 4H, C₆H₄), 7.65 (m, 1H, C₄H₃S), 6.88–6.78 (m, 2H, C₄H₃S), 5.44 (br t, 1H, C₂O₂NH), 3.32–3.22 (d, 2H, NHCH₂). ¹³C NMR (126 MHz, DMSO-d₆): δ 172.3, 168.1, 168.1, 141.9, 136.4, 133.2, 131.8, 131.2, 130.1, 129.8, 129.7, 128.9, 128.5, 51.9, 42.7.

4.1.2.16. 2-(2-Carboxy-1-(4-methoxyphenyl)ethyl)-1,3-dioxoisindoline-5-carboxylic acid (C-1). Yield: 85%, mp 100–2 °C FT IR (ν cm⁻¹): 3398–2950 (OH), 3071 (CH sp²), 1775_{asym}, 1702_{sym} (NC₂O₂), 1605_{asym}, 1359_{sym} (C=O), 1245 (C-O), 1172 (C-N). ¹H NMR (500 MHz, DMSO-d₆): δ 13.25 (s, 1H, COOH), 11.50 (s, 1H, C₆H₃COOH) 8.33 (s, 1H, C₆H₃), 8.30 (s, 1H, C₆H₃), 8.10 (s, 1H, C₆H₃), 7.85–7.83 (m, 2H, C₆H₄), 7.52–7.50 (m, 2H, C₆H₄), 5.89 (br t, 1H, C₂O₂NH), 3.80 (s, 3H, C₆H₄OCH₃), 3.51–3.45 (d, 2H, NHCH₂). ¹³C NMR (126 MHz, DMSO-d₆): δ 172.3, 169.9, 168.3, 168.3, 162.1, 141.2, 139.7, 136.2, 136.8, 135.6, 133.1, 130.9, 130.6, 130.5, 119.8, 119.6, 60.2, 55.1, 44.3.

4.1.2.17. 2-(2-Carboxy-1-(p-tolyl)ethyl)-1,3-dioxoisindoline-5-carboxylic acid (C-2). Yield: 85%, mp 112–5 °C, FT IR (ν cm⁻¹): 3398–2950 (OH), 3071 (CH sp²), 1775_{asym}, 1702_{sym} (NC₂O₂), 1605_{asym}, 1359_{sym} (C=O), 1245 (C-O), 1172 (C-N). ¹H NMR (500 MHz, DMSO-d₆): δ 13.30 (s, 1H, COOH), 11.57 (s, 1H, C₆H₃COOH) 8.31 (s, 1H, C₆H₃), 8.29 (s, 1H, C₆H₃), 8.15 (s, 1H, C₆H₃), 7.95–7.93 (m, 2H, C₆H₄), 7.71–7.69 (m, 2H, C₆H₄), 5.88 (br t, 1H, C₂O₂NH), 3.56–3.44 (d, 2H, NHCH₂), 2.49 (s, 3H, C₆H₄CH₃). ¹³C NMR (126 MHz, DMSO-d₆): δ 172.9, 169.8, 167.8, 167.8, 142.5, 141.5, 140.8, 140.6, 139.5, 136.6, 134.6, 134.3, 133.3, 132.0, 128.6, 128.4, 55.2, 44.0, 25.8.

4.1.2.18. 2-(2-Carboxy-1-(4-ethylphenyl)ethyl)-1,3-dioxoisindoline-5-carboxylic acid (C-3). Yield: 85%, mp 116–8 °C, FT IR (ν cm⁻¹): 3415–2970 (OH), 3033 (CH sp²), 1774_{asym}, 1695_{sym} (NC₂O₂), 1625_{asym}, 1380_{sym} (C=O), 1248 (C-O), 1164 (C-N). ¹H NMR (500 MHz, DMSO-d₆): δ 13.23 (s, 1H, COOH), 11.49 (s, 1H, C₆H₃COOH) 8.33 (s, 1H, C₆H₃), 8.30 (s, 1H, C₆H₃), 8.10 (s, 1H, C₆H₃), 7.99–7.97 (m, 2H, C₆H₄), 7.81–7.79 (m, 2H, C₆H₄), 5.90 (br t, 1H, C₂O₂NH), 3.44–3.38 (d, 2H, NHCH₂), 2.38 (q, 2H, C₆H₄CH₂CH₃), 1.27 (t, 3H, C₆H₄CH₂CH₃).

^{13}C NMR (126 MHz, DMSO- d_6): δ 172.1, 169.1, 168.1, 168.1, 142.9, 141.1, 140.3, 140.1, 139.3, 136.4, 134.1, 134.0, 133.5, 129.9, 129.6, 128.3, 54.9, 44.3, 31.7, 20.1.

4.1.2.19. 2-(2-Carboxy-1-(4-hydroxyphenyl)ethyl)-1,3-dioxoisindoline-5-carboxylic acid (C-4). Yield: 87%, mp 128–0 °C FT IR (ν cm^{-1}): 3410–2905 (OH), 3011 (CH sp^2), 1763_{asym}, 1702_{sym} (NC_2O_2), 1619_{asym}, 1379_{sym} (C=O), 1238 (C-O), 1170 (C-N). ^1H NMR (500 MHz, DMSO- d_6) δ 12.99 (s, 1H, COOH), 11.3 (s, 1H, $\text{C}_6\text{H}_3\text{COOH}$), 8.31 (s, 1H, C_6H_3), 8.30 (s, 1H, C_6H_3), 8.01 (s, 1H, C_6H_3), 7.87–7.85 (m, 2H, C_6H_4), 7.25–7.15 (m, 2H, C_6H_4), 5.81 (s, 1H, $\text{C}_6\text{H}_4\text{OH}$), 5.62 (br t, 1H, $\text{C}_2\text{O}_2\text{NH}$), 3.42–3.31 (d, 2H, NHCH_2). ^{13}C NMR (126 MHz, DMSO- d_6): δ 172.3, 169.0, 167.2, 167.2, 157.4, 139.9, 138.8, 134.8, 133.4, 132.7, 132.5, 129.0, 123.2, 122.1, 115.7, 115.2, 50.1, 39.8.

4.1.2.20. 2-(2-Carboxy-1-(4-nitrophenyl)ethyl)-1,3-dioxoisindoline-5-carboxylic acid (C-5). Yield: 85%, mp 154–6 °C, FT IR (ν cm^{-1}): 3395–2926 (OH), 3017 (CH sp^2), 1775_{asym}, 1698_{sym} (NC_2O_2), 1619_{asym}, 1363_{sym} (C=O), 1516 (NO_2), 1281 (C-O), 1172 (C-N). ^1H NMR (500 MHz, DMSO- d_6): δ 13.10 (s, 1H, COOH), 11.5 (s, 1H, $\text{C}_6\text{H}_3\text{COOH}$), 8.35 (s, 1H, C_6H_3), 8.33 (s, 1H, C_6H_3), 8.22–8.18 (m, 2H, C_6H_4), 8.05 (s, 1H, C_6H_3), 7.96–7.87 (m, 2H, C_6H_4), 5.89 (br t, 1H, $\text{C}_2\text{O}_2\text{NH}$), 3.54–3.28 (d, 2H, NHCH_2). ^{13}C NMR (126 MHz, DMSO- d_6): δ 171.7, 169.8, 167.6, 167.6, 148.7, 138.8, 138.1, 136.2, 135.3, 135.2, 134.2, 134.0, 133.0, 132.1, 131.0, 123.3, 50.2, 40.47.

4.1.2.21. 2-(2-Carboxy-1-(4-fluorophenyl)ethyl)-1,3-dioxoisindoline-5-carboxylic acid (C-6). Yield: 86%, mp 165–8 °C, FT IR (ν cm^{-1}): 3420–2898 (OH), 3013 (CH sp^2), 1776_{asym}, 1695_{sym} (NC_2O_2), 1624_{asym}, 1336_{sym} (C=O), 1280 (C-O), 1160 (C-N), 790 (C-F). ^1H NMR (500 MHz, DMSO- d_6) δ 13.04 (s, 1H, COOH), 11.57 (s, 1H, $\text{C}_6\text{H}_3\text{COOH}$), 8.34 (s, 1H, C_6H_3), 8.20 (s, 1H, C_6H_3), 8.01 (s, 1H, C_6H_3), 7.77–7.61 (m, 2H, C_6H_4), 7.40–7.32 (m, 2H, C_6H_4), 5.71 (br t, 1H, $\text{C}_2\text{O}_2\text{NH}$), 3.48–3.30 (d, 2H, NHCH_2). ^{13}C NMR (126 MHz, DMSO- d_6): δ 172.1, 169.1, 167.2, 167.2, 161.1, 140.2, 136.1, 135.9, 135.2, 134.7, 133.8, 133.6, 132.2, 116.8, 115.9, 50.5, 40.3.

4.1.2.22. 2-(2-Carboxy-1-(4-chlorophenyl)ethyl)-1,3-dioxoisindoline-5-carboxylic acid (C-7). Yield: 88%, mp 142–6 °C, FT IR (ν cm^{-1}): 3467–2900 (OH), 3037 (CH sp^2), 1775_{asym}, 1701_{sym} (NC_2O_2), 1626_{asym}, 1359_{sym} (C=O), 1275 (C-O), 1154 (C-N), 725 (C-Cl). ^1H NMR (500 MHz, DMSO- d_6) δ 13.10 (s, 1H, COOH), 11.54 (s, 1H, $\text{C}_6\text{H}_3\text{COOH}$), 8.32 (s, 1H, C_6H_3), 8.19 (s, 1H, C_6H_3), 8.07 (s, 1H, C_6H_3), 7.86–7.80 (m, 2H, C_6H_4), 7.45–7.36 (m, 2H, C_6H_4), 5.71 (br t, 1H, $\text{C}_2\text{O}_2\text{NH}$), 3.47–3.31 (d, 2H, NHCH_2). ^{13}C NMR (126 MHz, DMSO- d_6): δ 173.1, 171.3, 169.4, 169.4, 148.3, 141.9, 140.2, 139.5, 138.6, 138.0, 135.1, 134.8, 134.6, 134.5, 133.8, 130.2, 54.7, 44.6.

4.1.2.23. 2-(1-(4-bromophenyl)-2-carboxyethyl)-1,3-dioxoisindoline-5-carboxylic acid (C-8). Yield: 80%, mp 166–8 °C, FT IR (ν cm^{-1}): 3430–2940 (OH), 3028 (CH sp^2), 1775_{asym}, 1696_{sym} (NC_2O_2), 1637_{asym}, 1358_{sym} (C=O), 1280 (C-O), 1169 (C-N), 699 (C-Br). ^1H NMR (500 MHz, DMSO- d_6) δ 13.30 (s, 1H, COOH), 11.53 (s, 1H, $\text{C}_6\text{H}_3\text{COOH}$), 8.33 (m, 1H, C_6H_3), 8.20 (s, 1H, C_6H_3), 8.16 (m, 1H, C_6H_3), 7.96–7.88 (m, 2H, C_6H_4), 7.58–7.39 (m, 2H, C_6H_4), 5.64 (br t, 1H, $\text{C}_2\text{O}_2\text{NH}$), 3.46–3.31 (d, 2H, NHCH_2). ^{13}C NMR (126 MHz, DMSO- d_6): δ 172.3, 169.9, 166.8, 166.8, 143.2, 138.5, 137.5, 137.0, 136.0, 135.4, 133.0, 132.4, 132.0, 131.9, 130.5, 129.5, 50.5, 40.3.

4.1.2.24. 2-(2-Carboxy-1-(7-nitro-2,3-dihydrobenzo[b][1,4]dioxin-6-yl)ethyl)-1,3-dioxoisindoline-5-carboxylic acid (C-9). Yield: 84%, mp 172–4 °C, FT IR (ν cm^{-1}): 3421–2977 (OH), 2999 (CH sp^2), 1775_{asym}, 1702_{sym} (NC_2O_2), 1606_{asym}, 1360_{sym} (C=O), 1256 (C-O), 1157 (C-N). ^1H NMR (500 MHz, DMSO- d_6): δ 12.42 (s, 1H, COOH), 11.48 (s, 1H, $\text{C}_6\text{H}_3\text{COOH}$), 8.34 (s, 1H, C_6H_3), 8.31 (s, 1H, C_6H_3), 8.01 (s,

1H, C_6H_3), 7.77 (s, 1H, C_6H_3), 7.68 (s, 1H, C_6H_3), 5.71 (br t, 1H, $\text{C}_2\text{O}_2\text{NH}$), 4.19 (m, 4H, $\text{C}_6\text{H}_3\text{O}_2\text{C}_2\text{H}_4$), 3.66–3.12 (d, 2H, NHCH_2). ^{13}C NMR (126 MHz, DMSO- d_6): δ 172.3, 169.0, 167.8, 167.8, 156.9, 152.8, 149.1, 143.9, 142.8, 139.3, 131.1, 129.3, 129.1, 126.2, 124.3, 69.8, 69.8, 49.3, 40.9.

4.1.2.25. 2-(2-Carboxy-1-(2,3-dihydrobenzo[b][1,4]dioxin-6-yl)ethyl)-1,3-dioxoisindoline-5-carboxylic acid (C-10). Yield: 80%, mp 161–4 °C, FT IR (ν cm^{-1}): 3421–2929 (OH), 2990 (CH sp^2), 1763_{asym}, 1697_{sym} (NC_2O_2), 1619_{asym}, 1356_{sym} (C=O), 1250 (C-O), 1147 (C-N). ^1H NMR (500 MHz, DMSO- d_6): δ 12.98 (s, 1H, COOH), 11.38 (s, 1H, $\text{C}_6\text{H}_3\text{COOH}$), 8.34 (s, 1H, C_6H_3), 8.29 (s, 1H, C_6H_3), 8.09 (s, 1H, C_6H_3), 7.46 (s, 1H, C_6H_3), 7.19 (s, 1H, C_6H_3), 7.10 (s, 1H, C_6H_3), 5.61 (br t, 1H, $\text{C}_2\text{O}_2\text{NH}$), 4.20 (m, 4H, $\text{C}_6\text{H}_3\text{O}_2\text{C}_2\text{H}_4$), 3.42–3.22 (d, 2H, NHCH_2). ^{13}C NMR (126 MHz, DMSO- d_6): δ 172.4, 169.4, 168.1, 168.1, 147.2, 146.9, 143.6, 134.9, 133.0, 131.9, 130.8, 129.6, 123.1, 120.4, 119.2, 116.0, 64.8, 64.8, 50.1, 40.0.

4.1.2.26. 2-(2-Carboxy-1-(naphthalen-2-yl)ethyl)-1,3-dioxoisindoline-5-carboxylic acid (C-11). Yield: 85%, mp 142–4 °C, FT IR (ν cm^{-1}): 3400–2947 (OH), 3062 (CH sp^2), 1776_{asym}, 1699_{sym} (NC_2O_2), 1622_{asym}, 1362_{sym} (C=O), 1255 (C-O), 1173 (C-N). ^1H NMR (500 MHz, DMSO- d_6): δ 13.27 (s, 1H, COOH), 11.56 (s, 1H, $\text{C}_6\text{H}_3\text{COOH}$), 8.33 (m, 1H, C_6H_3), 8.30 (m, 1H, C_6H_3), 8.01 (m, 1H, C_6H_3), 7.99 (m, 1H, C_8H_7), 7.82 (m, 1H, C_8H_7), 7.61 (m, 1H, C_8H_7), 7.58–7.45 (m, 1H, C_8H_7), 7.28 (d, 1H, C_8H_7), 5.89 (br t, 1H, $\text{C}_2\text{O}_2\text{NH}$), 3.57–3.49 (d, 2H, NHCH_2). ^{13}C NMR (126 MHz, DMSO- d_6): δ 172.3, 168.9, 167.2, 167.2, 144.3, 136.6, 136.5, 136.4, 136.3, 135.6, 135.5, 134.8, 133.4, 132.8, 132.0, 130.9, 129.1, 128.2, 126.0, 124.3, 50.9, 40.3.

4.1.2.27. 2-(1-([1,1'-biphenyl]-4-yl)-2-carboxyethyl)-1,3-dioxoisindoline-5-carboxylic acid (C-12). Yield: 87%, mp 156–8 °C, FT IR (ν cm^{-1}): 3422–3120 (OH), 3007 (CH sp^2), 1775_{asym}, 1698_{sym} (NC_2O_2), 1625_{asym}, 1360_{sym} (C=O), 1223 (C-O), 1170 (C-N). ^1H NMR (500 MHz, DMSO- d_6): δ 13.13 (s, 1H, COOH), 11.58 (s, 1H, $\text{C}_6\text{H}_3\text{COOH}$), 8.36 (m, 1H, C_6H_3), 8.22 (s, 1H, C_6H_3), 8.01 (s, 1H, C_6H_3), 7.79–7.31 (m, 9H, C_{12}H_9), 5.77 (br t, 1H, $\text{C}_2\text{O}_2\text{NH}$), 3.50–3.39 (d, 2H, NHCH_2). ^{13}C NMR (126 MHz, DMSO- d_6): δ 172.3, 169.3, 166.8, 166.8, 143.2, 142.2, 140.5, 140.4, 139.6, 138.2, 136.9, 136.5, 135.5, 134.8, 133.7, 133.5, 132.2, 129.6, 128.3, 127.3, 126.5, 124.5, 50.5, 40.3.

4.1.2.28. 2-(2-Carboxy-1-(2-nitrophenyl)ethyl)-1,3-dioxoisindoline-5-carboxylic acid (C-13). Yield: 85%, mp 131–4 °C, FT IR (ν cm^{-1}): 3395–2926 (OH), 3017 (CH sp^2), 1775_{asym}, 1698_{sym} (NC_2O_2), 1619_{asym}, 1363_{sym} (C=O), 1516 (NO_2), 1281 (C-O), 1172 (C-N). ^1H NMR (500 MHz, DMSO- d_6): δ 13.09 (s, 1H, COOH), 11.58 (s, 1H, $\text{C}_6\text{H}_3\text{COOH}$), 8.33 (s, 1H, C_6H_3), 8.30 (s, 1H, C_6H_3), 8.20–8.18 (m, 2H, C_6H_4), 8.10 (s, 1H, C_6H_3), 7.99–7.92 (m, 2H, C_6H_4), 5.82 (br t, 1H, $\text{C}_2\text{O}_2\text{NH}$), 3.48–3.40 (d, 2H, NHCH_2). ^{13}C NMR (126 MHz, DMSO- d_6): δ 172.2, 169.0, 167.6, 167.6, 149.7, 138.6, 138.3, 136.4, 135.8, 135.4, 134.3, 134.0, 133.8, 132.6, 131.7, 123.2, 51.3, 41.4.

4.1.2.29. 2-(2-Carboxy-1-(furan-2-yl)ethyl)-1,3-dioxoisindoline-5-carboxylic acid (C-14). Yield: 80%, mp 151–4 °C, FT IR (ν cm^{-1}): 3421–2899 (OH), 2990 (CH sp^2), 1762_{asym}, 1720_{sym} (NC_2O_2), 1620_{asym}, 1357_{sym} (C=O), 1255 (C-O), 1177 (C-N). ^1H NMR (500 MHz, DMSO- d_6): δ 12.60 (s, 1H, COOH), 11.10 (s, 1H, $\text{C}_6\text{H}_3\text{COOH}$), 8.32 (s, 1H, C_6H_3), 8.24 (s, 1H, C_6H_3), 7.58 (s, 1H, C_6H_3), 7.77 (m, 1H, $\text{C}_4\text{H}_3\text{O}$), 7.01–6.69 (m, 2H, $\text{C}_4\text{H}_3\text{O}$), 5.59 (br t, 1H, $\text{C}_2\text{O}_2\text{NH}$), 3.31–3.02 (d, 2H, NHCH_2), 2.43 (s, 3H, $\text{C}_6\text{H}_3\text{CH}_3$). ^{13}C NMR (126 MHz, DMSO- d_6): δ 172.0, 169.3, 168.1, 168.1, 156.0, 146.4, 143.9, 142.1, 137.2, 135.4, 129.7, 124.5, 119.4, 117.1, 50.9, 40.9.

4.1.2.30. 2-(2-Carboxy-1-(thiophen-2-yl)ethyl)-1,3-dioxoisindoline-5-carboxylic acid (C-15). Yield: 88%, mp 139–1 °C, FT IR (ν cm^{-1}):

3402–2945 (OH), 3010 (CH₂ sp²), 1763_{asym}, 1698_{sym} (NC₂O₂), 1618_{asym}, 1359_{sym} (C=O), 1259 (C-O), 1175 (C-N). ¹H NMR (500 MHz, DMSO-*d*₆): δ 11.99 (s, 1H, COOH), 10.10 (s, 1H, C₆H₃COOH), 8.34 (s, 1H, C₆H₃), 8.31 (s, 1H, C₆H₃), 8.11 (s, 1H, C₆H₃), 7.51 (m, 1H, C₄H₃S), 7.01–6.99 (m, 2H, C₄H₃O), 5.69 (br t, 1H, C₂O₂NH), 3.40–3.31 (d, 2H, NHCH₂). ¹³C NMR (126 MHz, DMSO-*d*₆): δ 172.3, 169.4, 168.0, 168.0, 141.0, 136.7, 133.3, 130.1, 129.8, 129.7, 129.4, 129.1, 128.8, 128.3, 51.3, 41.6.

4.1.2.31. 3-(4-methoxyphenyl)-3-(5-methyl-1,3-dioxoisindolin-2-yl) propanoic acid (D-1). Yield: 85%, mp 107–9 °C, FT IR (ν cm⁻¹): 3410–2904 (OH), 3042 (CH sp²), 1766_{asym}, 1698_{sym} (NC₂O₂), 1609_{asym}, 1380_{sym} (C=O), 1247 (C-O), 1175 (C-N). ¹H NMR (500 MHz, DMSO-*d*₆): δ 12.46 (s, 1H, COOH), 7.73 (s, 1H, C₆H₃), 7.71 (s, 1H, C₆H₃), 7.49 (s, 1H, C₆H₃), 7.34–7.32 (m, 2H, C₆H₄), 6.89–6.87 (m, 2H, C₆H₄), 5.58 (br t, 1H, C₂O₂NH), 3.72 (s, C₆H₄OCH₃), 3.44–3.40 (d, 2H, NHCH₂), 2.09 (s, 3H, CH₃). ¹³C NMR (126 MHz, DMSO-*d*₆): δ 172.3, 168.4, 168.4, 157.2, 140.0, 138.2, 132.2, 131.9, 131.2, 129.1, 129.0, 123.5, 123.5, 118.7, 115.2, 55.6, 50.0, 40.34, 21.03.

4.1.2.32. 3-(5-Methyl-1,3-dioxoisindolin-2-yl)-3-(*p*-tolyl)propanoic acid (D-2). Yield: 88%, mp 116–8 °C, FT IR (ν cm⁻¹): 3400–2888 (OH), 3029 (CH sp²), 1767_{asym}, 1697_{sym} (NC₂O₂), 1614_{asym}, 1379_{sym} (C=O), 1254 (C-O), 1168 (C-N). ¹H NMR (500 MHz, DMSO-*d*₆): δ 12.43 (s, 1H, COOH), 7.96 (s, 1H, C₆H₃), 7.88 (s, 1H, C₆H₃), 7.65 (s, 1H, C₆H₃), 7.29–7.27 (m, 2H, C₆H₄), 7.13–7.11 (m, 2H, C₆H₄), 5.64 (br t, 1H, C₂O₂NH), 3.22–3.20 (d, 2H, NHCH₂), 2.02 (s, 6H, C₆H₃CH₃, C₆H₄CH₃). ¹³C NMR (126 MHz, DMSO-*d*₆): δ 172.1, 168.7, 168.7, 142.0, 141.4, 137.4, 135.1, 131.9, 129.6, 129.0, 126.2, 124.9, 123.7, 123.2, 50.4, 40.13, 21.7, 21.5.

4.1.2.33. 3-(4-ethylphenyl)-3-(5-methyl-1,3-dioxoisindolin-2-yl) propanoic acid (D-3). Yield: 87%, mp 114–6 °C, FT IR (ν cm⁻¹): 3415–2940 (OH), 2989 (CH sp²), 1767_{asym}, 1700_{sym} (NC₂O₂), 1617_{asym}, 1380_{sym} (C=O), 1277 (C-O), 1167 (C-N). ¹H NMR (500 MHz, DMSO-*d*₆): δ 12.17 (s, 1H, COOH), 7.73 (s, 1H, C₆H₃), 7.71 (s, 1H, C₆H₃), 7.62 (s, 1H, C₆H₃), 7.31–7.29 (m, 2H, C₆H₄), 7.17–7.15 (m, 2H, C₆H₄), 5.61 (br t, 1H, C₂O₂NH), 3.44–3.38 (d, 2H, NHCH₂), 2.44 (q, 2H, C₆H₄CH₂CH₃), 2.07 (s, 3H, CH₃), 1.16 (t, 3H, C₆H₄CH₂CH₃). ¹³C NMR (126 MHz, DMSO-*d*₆): δ 171.9, 167.9, 167.9, 146.1, 143.9, 136.8, 136.3, 128.9, 128.4, 127.8, 127.4, 124.0, 123.5, 50.5, 40.3, 36.3, 28.2, 21.7, 15.9.

4.1.2.34. 3-(4-hydroxyphenyl)-3-(5-methyl-1,3-dioxoisindolin-2-yl) propanoic acid (D-4). Yield: 85%, mp 131–3 °C, FT IR (ν cm⁻¹): 3400–2915 (OH), 3057 (CH sp²), 1764_{asym}, 1700_{sym} (NC₂O₂), 1606_{asym}, 1354_{sym} (C=O), 1254 (C-O), 1170 (C-N). ¹H NMR (500 MHz, DMSO-*d*₆): δ 12.47 (s, 1H, COOH), 7.99 (s, 1H, C₆H₃), 7.96 (s, 1H, C₆H₃), 7.76 (s, 1H, C₆H₃), 7.16–7.19 (m, 2H, C₆H₄), 6.87–6.80 (m, 2H, C₆H₄), 6.01 (s, 1H, C₆H₄OH), 5.56 (br t, 1H, C₂O₂NH), 3.32–3.30 (d, 2H, NHCH₂), 2.11 (s, 3H, CH₃). ¹³C NMR (126 MHz, DMSO-*d*₆): δ 172.4, 168.8, 168.8, 159.2, 143.2, 138.4, 136.1, 133.1, 131.0, 130.0, 129.1, 129.0, 119.4, 119.0, 52.0, 41.2, 21.3.

4.1.2.35. 3-(5-Methyl-1,3-dioxoisindolin-2-yl)-3-(4-nitrophenyl) propanoic acid (D-5). Yield: 88%, mp 126–8 °C, FT IR (ν cm⁻¹): 3390–2960 (OH), 3065 (CH sp²), 1765_{asym}, 1701_{sym} (NC₂O₂), 1603_{asym}, 1340_{sym} (C=O), 1540 (NO₂), 1223 (C-O), 1172 (C-N). ¹H NMR (500 MHz, DMSO-*d*₆): δ 12.68 (s, 1H, COOH), 8.19–8.17 (m, 2H, C₆H₄), 7.98 (s, 1H, C₆H₃), 7.88 (s, 1H, C₆H₃), 7.74 (s, 1H, C₆H₃), 7.66–7.64 (m, 2H, C₆H₄), 5.77 (br t, 1H, C₂O₂NH), 3.30–3.24 (d, 2H, NHCH₂), 2.44 (s, 3H, CH₃). ¹³C NMR (126 MHz, DMSO-*d*₆): δ 172.3, 168.4, 168.4, 149.1, 147.3, 143.1, 136.1, 132.2, 131.1, 130.4, 130.1, 123.6, 123.5, 123.5, 123.4, 50.4, 39.7, 21.7.

4.1.2.36. 3-(4-fluorophenyl)-3-(5-methyl-1,3-dioxoisindolin-2-yl) propanoic acid (D-6). Yield: 89%, mp 136–8 °C, FT IR (ν cm⁻¹): 3388–2899 (OH), 3054 (CH sp²), 1767_{asym}, 1698_{sym} (NC₂O₂), 1604_{asym}, 1355_{sym} (C=O), 1227 (C-O), 1160 (C-N), 884 (C-F). ¹H NMR (500 MHz, DMSO-*d*₆): δ 12.49 (s, 1H, COOH), 7.85 (s, 1H, C₆H₃), 7.83 (s, 1H, C₆H₃), 7.76 (s, 1H, C₆H₃), 7.30–7.29 (m, 2H, C₆H₄), 7.13–7.11 (m, 2H, C₆H₄), 5.64 (br t, 1H, C₂O₂NH), 3.42–3.32 (d, 2H, NHCH₂), 2.12 (s, 3H, CH₃). ¹³C NMR (126 MHz, DMSO-*d*₆): δ 171.9, 167.9, 167.4, 162.4, 146.1, 141.1, 132.6, 132.1, 130.4, 129.3, 129.2, 124.6, 124.2, 116.8, 116.7, 50.1, 41.2, 21.8.

4.1.2.37. 3-(4-chlorophenyl)-3-(5-methyl-1,3-dioxoisindolin-2-yl) propanoic acid (D-7). Yield: 85%, mp 133–5 °C, FT IR (ν cm⁻¹): 3400–2970 (OH), 3056 (CH sp²), 1765_{asym}, 1699_{sym} (NC₂O₂), 1614_{asym}, 1378_{sym} (C=O), 1283 (C-O), 1171 (C-N), 839 (C-Cl). ¹H NMR (500 MHz, DMSO-*d*₆): δ 12.41 (s, 1H, COOH), 7.72 (s, 1H, C₆H₃), 7.69 (s, 1H, C₆H₃), 7.65 (s, 1H, C₆H₃), 7.52–7.50 (m, 2H, C₆H₄), 7.40–7.37 (m, 2H, C₆H₄), 5.65 (br t, 1H, C₂O₂NH), 3.38–3.19 (d, 2H, NHCH₂), 2.43 (s, 3H, CH₃). ¹³C NMR (126 MHz, DMSO-*d*₆): δ 172.3, 167.2, 167.2, 145.7, 141.4, 141.1, 138.8, 136.2, 134.6, 134.3, 132.1, 132.0, 129.0, 128.4, 50.2, 40.7, 21.8.

4.1.2.38. 3-(4-bromophenyl)-3-(5-methyl-1,3-dioxoisindolin-2-yl) propanoic acid (D-8). Yield: 84%, mp 142–5 °C, FT IR (ν cm⁻¹): 3410–2910 (OH), 3055 (CH sp²), 1765_{asym}, 1699_{sym} (NC₂O₂), 1617_{asym}, 1377_{sym} (C=O), 1205 (C-O), 1171 (C-N), 786 (C-Br). ¹H NMR (500 MHz, DMSO-*d*₆): δ 12.48 (s, 1H, COOH), 7.76 (s, 1H, C₆H₃), 7.71 (s, 1H, C₆H₃), 7.64–7.60 (m, 2H, C₆H₄), 7.51 (s, 1H, C₆H₃), 7.35–7.33 (m, 2H, C₆H₄), 5.62 (br t, 1H, C₂O₂NH), 3.37–3.35 (d, 2H, NHCH₂), 2.44 (s, 3H, CH₃). ¹³C NMR (126 MHz, DMSO-*d*₆): δ 172.2, 168.1, 168.1, 145.5, 144.9, 136.5, 135.9, 132.2, 131.8, 131.8, 130.4, 129.0, 128.7, 124.6, 124.4, 13.7, 50.5, 40.8, 21.7.

4.1.2.39. 3-(5-Methyl-1,3-dioxoisindolin-2-yl)-3-(7-nitro-2,3-dihydrobenzo[*b*] [1,4]dioxin-6-yl)propanoic acid (D-9). Yield: 88%, mp 177–9 °C, FT IR (ν cm⁻¹): 3380–2988 (OH), 3052 (CH sp²), 1764_{asym}, 1703_{sym} (NC₂O₂), 1615_{asym}, 1356_{sym} (C=O), 1521 (NO₂), 1256 (C-O), 1160 (C-N). ¹H NMR (500 MHz, DMSO-*d*₆): δ 12.42 (s, 1H, COOH), 7.78 (s, 1H, C₆H₃), 7.76 (s, 1H, C₆H₃), 7.62 (s, 1H, C₆H₃), 7.50 (s, 1H, C₆H₃), 7.24 (s, 1H, C₆H₃), 5.54 (br t, 1H, C₂O₂NH), 3.99 (m, 4H, C₆H₃O₂C₂H₄), 3.11–2.99 (d, 2H, NHCH₂), 2.48 (s, 3H, CH₃). ¹³C NMR (126 MHz, DMSO-*d*₆): δ 171.9, 168.7, 168.7, 154.9, 152.2, 148.9, 143.1, 142.4, 138.4, 130.2, 129.3, 129.1, 126.2, 123.2, 69.4, 69.4, 47.6, 40.3, 21.4.

4.1.2.40. 3-(2,3-dihydrobenzo[*b*] [1,4]dioxin-6-yl)-3-(5-methyl-1,3-dioxoisindolin-2-yl)propanoic acid (D-10). Yield: 85%, mp 165–8 °C, FT IR (ν cm⁻¹): 3423–2980 (OH), 3042 (CH sp²), 1766_{asym}, 1698_{sym} (NC₂O₂), 1611_{asym}, 1380_{sym} (C=O), 1250 (C-O), 1170 (C-N). ¹H NMR (500 MHz, DMSO-*d*₆): δ 12.39 (s, 1H, COOH), 7.68 (s, 1H, C₆H₃), 7.60 (s, 1H, C₆H₃), 7.57 (s, 1H, C₆H₃), 6.87 (s, 1H, C₆H₃), 6.76 (s, 1H, C₆H₃), 6.70 (s, 1H, C₆H₃), 5.54 (br t, 1H, C₂O₂NH), 4.22 (m, 4H, C₆H₃O₂C₂H₄), 3.01–2.99 (d, 2H, NHCH₂), 2.47 (s, 3H, CH₃). ¹³C NMR (126 MHz, DMSO-*d*₆): δ 171.1, 167.9, 167.9, 147.7, 147.7, 143.1, 134.7, 133.4, 132.2, 130.1, 129.2, 122.2, 117.4, 116.2, 114.0, 65.1, 65.1, 50.5, 40.6, 21.1.

4.1.2.41. 3-(5-Methyl-1,3-dioxoisindolin-2-yl)-3-(naphthalen-2-yl) propanoic acid (D-11). Yield: 88%, mp 142–4 °C, FT IR (ν cm⁻¹): 3390–2947 (OH), 3042 (CH sp²), 1765_{asym}, 1700_{sym} (NC₂O₂), 1616_{asym}, 1354_{sym} (C=O), 1259 (C-O), 1194 (C-N). ¹H NMR (500 MHz, DMSO-*d*₆): δ 11.37 (s, 1H, COOH), 8.12 (m, 1H, C₈H₇), 8.08 (m, 1H, C₆H₃), 8.06 (m, 1H, C₈H₇), 8.01 (m, 1H, C₈H₇), 8.00 (m, 1H, C₆H₃), 7.99–7.61 (m, 1H, C₈H₇), 7.28 (d, 1H, C₈H₇), 5.871 (br t, 1H, C₂O₂NH), 3.62–3.45 (d, 2H, NHCH₂), 2.38 (s, 3H, CH₃). ¹³C NMR (126 MHz,

DMSO- d_6): δ 172.34, 168.4, 168.4, 145.1, 144.7, 136.6, 133.6, 133.1, 132.4, 132.2, 131.3, 130.4, 130.2, 129.8, 129.7, 129.3, 128.9, 128.7, 128.5, 50.5, 40.3, 21.4.

4.1.2.42. 3-([1,1'-biphenyl]-4-yl)-3-(5-methyl-1,3-dioxoisindolin-2-yl)propanoic acid (D-12). Yield: 85%, mp 152–5 °C, FT IR (ν cm^{-1}): 3410–2964 (OH), 3054 (CH sp^2), 1767_{asym}, 1700_{sym} (NC_2O_2), 1620_{asym}, 1379_{sym} (C=O), 1279 (C-O), 1169 (C-N). ^1H NMR (500 MHz, DMSO- d_6): δ 12.49 (s, 1H, COOH), 7.85 (s, 1H, C_6H_3), 7.82 (s, 1H, C_6H_3), 7.70 (s, 1H, C_6H_3), 7.54–7.12 (m, 9H, C_{12}H_9), 5.64 (br t, 1H, $\text{C}_2\text{O}_2\text{NH}$), 3.48–3.30 (d, 2H, NHCH_2), 2.23 (s, 3H, CH_3). ^{13}C NMR (126 MHz, DMSO- d_6): δ 172.4, 168.1, 168.1, 150.2, 147.3, 133.1, 132.9, 132.8, 132.7, 131.3, 131.2, 131.0, 130.8, 130.6, 130.5, 130.5, 130.4, 130.1, 130.0, 54.2, 44.4, 22.2.

4.1.2.43. 3-(5-Methyl-1,3-dioxoisindolin-2-yl)-3-(2-nitrophenyl)propanoic acid (D-13). Yield: 85%, mp 154–6 °C, FT IR (ν cm^{-1}): 3390–2995 (OH), 3056 (CH sp^2), 1765_{asym}, 1704_{sym} (NC_2O_2), 1609_{asym}, 1380_{sym} (C=O), 1571 (NO_2), 1266 (C-O), 1186 (C-N). ^1H NMR (500 MHz, DMSO- d_6): δ 12.68 (s, 1H, COOH), 8.10–8.08 (m, 2H, C_6H_4), 8.00 (s, 1H, C_6H_3), 7.93 (s, 1H, C_6H_3), 7.81 (s, 1H, C_6H_3), 7.71–7.68 (m, 2H, C_6H_4), 5.69 (br t, 1H, $\text{C}_2\text{O}_2\text{NH}$), 3.21–3.19 (d, 2H, NHCH_2), 2.39 (s, 3H, CH_3). ^{13}C NMR (126 MHz, DMSO- d_6): δ 172.1, 168.7, 168.7, 150.3, 147.8, 143.5, 136.5, 132.1, 131.0, 130.3, 130.3, 123.5, 123.4, 123.8, 123.6, 50.7, 40.1, 21.2.

4.1.2.44. 3-(Furan-2-yl)-3-(5-methyl-1,3-dioxoisindolin-2-yl)propanoic acid (D-14). Yield: 85%, mp 142–5 °C, FT IR (ν cm^{-1}): 3371–2895 (OH), 3042 (CH sp^2), 1769_{asym}, 1703_{sym} (NC_2O_2), 1624_{asym}, 1383_{sym} (C=O), 1250 (C-O), 1169 (C-N). ^1H NMR (500 MHz, DMSO- d_6): δ 12.12 (s, 1H, COOH), 7.71 (s, 1H, C_6H_3), 7.68 (s, 1H, C_6H_3), 7.65 (m, 1H, $\text{C}_4\text{H}_3\text{O}$), 7.58 (s, 1H, C_6H_3), 7.20–6.69 (m, 2H, $\text{C}_4\text{H}_3\text{O}$), 5.59 (br t, 1H, $\text{C}_2\text{O}_2\text{NH}$), 3.31–3.02 (d, 2H, NHCH_2), 2.43 (s, 3H, CH_3). ^{13}C NMR (126 MHz, DMSO- d_6): δ 172.1, 168.7, 168.7, 157.0, 145.4, 143.5, 141.8, 135.2, 133.4, 128.5, 123.6, 115.5, 116.3, 50.54, 40.7, 21.4.

4.1.2.45. 3-(5-Methyl-1,3-dioxoisindolin-2-yl)-3-(thiophen-2-yl)propanoic acid (D-15). Yield: 85%, mp 141–4 °C, FT IR (ν cm^{-1}): 3410–2907 (OH), 3052 (CH sp^2), 1764_{asym}, 1704_{sym} (NC_2O_2), 1613_{asym}, 1380_{sym} (C=O), 1280 (C-O), 1171 (C-N). ^1H NMR (500 MHz, DMSO- d_6): δ 12.12 (s, 1H, COOH), 7.86 (s, 1H, C_6H_3), 7.80 (s, 1H, C_6H_3), 7.65 (m, 1H, $\text{C}_4\text{H}_3\text{S}$), 7.67 (s, 1H, C_6H_3), 7.11–6.99 (m, 2H, $\text{C}_4\text{H}_3\text{O}$), 5.61 (br t, 1H, $\text{C}_2\text{O}_2\text{NH}$), 3.34–3.22 (d, 2H, NHCH_2), 2.40 (s, 3H, CH_3). ^{13}C NMR (126 MHz, DMSO- d_6): δ 172.3, 168.1, 168.1, 141.9, 136.4, 133.2, 130.1, 130.0, 129.8, 129.4, 129.1, 128.5, 128.4, 51.9, 41.0, 21.2.

4.2. Molecular docking

4.2.1. Receptors preparation

The crystal structure of *trans*-sialidase was retrieved from Protein Data Bank with PDB ID 1MS8 [10]. This protein exists co-crystallized with its natural substrate 3-deoxy-2,3-didehydro-*N*-acetylneuraminic acid (DANA), which is located in active sites of TcTS enzyme. The TcTS structure was prepared as receptor removing the ligand (DANA) and water molecules, for docking process. Vina [41] configuration file was generated by using the AutoDock [42] Tools software, and polar hydrogen and Gasteiger charges were added to finally get the file in PDBQT format. Then the location of the natural ligand was inspected to obtain the best grid box by using auto dock graphical interface. The first docking process was started with DANA (natural ligand) in order to obtain the most compromising size and space for active site of TcTS and several rounds of docking was carried out to obtain the following

final size space dimension, $x = 16 \text{ \AA}$, $y = 16 \text{ \AA}$ & $z = 16 \text{ \AA}$, and centre 40.881, 63.047 and -37.451 for x , y and z coordinates respectively. The binding energy of DANA obtained was used as a reference.

4.2.2. Ligands preparation

All compounds were drawn and energy minimized by using MarvinSketch software (www.chemaxon.com) and was saved as the mol2 file format. The hydrogens and Gasteiger charges were added by AutoDock tools, and change the file format mol2 to PDBQT format [41]. Then each compound was docked with Vina and best predicted binding affinity was determined and ranked according to reference DANA. The compounds with higher values than reference were considered as weak binding ligand and vice versa. Ligand interaction with amino acid and 2D & 3D interaction was produced by using Discovery Studio Client 2017 R [43].

4.3. In vitro trypanocidal assay

In vitro evaluation of all synthesized compounds were carried out using two strains of trypomastigotes of *T. cruzi*: NINOA and INC-5 by reported procedure, with slight modifications [44]. Blood infected with trypomastigotes from *T. cruzi* strains was obtained by cardiac puncture of infected NIH mice at peak of parasitemia, using heparin as an anticoagulant. Blood was treated with isotonic saline solution (NaCl 0.85%) to adjust the concentration of approximately 1×10^6 trypomastigotes/mL. The stock solutions (10 mg/mL) in dimethyl sulfoxide (DMSO) of all synthesized compounds and reference drugs were prepared. Subsequent dilutions were carried out with sterile distilled water. The test compounds concentration were adjusted to 10 $\mu\text{g/mL}$ dimethyl sulfoxide (DMSO) and the final concentration of DMSO in culture medium was adjusted below 1%. A solution of DMSO/ H_2O (1:99) was used as negative control. The assay was carried out in triplicate on 96 well microplate (Biofil JET) containing, 195 μL of infected blood and 5 μL of tested compounds per well. After determination of trypanocidal activity of all compounds, the compounds with percentage lysis $>50\%$ were selected to determine the lysis concentration of fifty percent population (LC_{50}). LC_{50} values were determined using Probit statistical analysis of the dose-response, and the results were expressed as the mean \pm standard deviation (SD). A negative control of lysis, wells with untreated blood trypomastigotes were used, and as a positive control, wells with reference drugs were used. The plates were incubated for 24 h at 4 °C to avoid the change to the epimastigotes phase. The bloodstream trypomastigotes were counted by Berner method [45]. Briefly, 5 μL of blood were spread on slides, covered with a coverslip, and flagellates were examined with an optical microscope at 40 \times magnification. Anti *T. cruzi* activity was expressed as lysis percentage by comparing the remaining trypomastigotes in each concentration with respect to the negative control group. The LC_{50} values were later converted in micromolar (μM) units.

4.4. Enzyme inhibition assay

4.4.1. Inhibition of sialylation of *N*-acetylglucosamine (LN)

Reaction mixtures of 20 μL containing 1 mM the of compounds A-4, A-11, A-14, B-4 B-11, B-14, C-4, C-11, C-14, D-4, D11, D-14 and 20 mM Tris-HCl pH 7 buffer, 30 mM NaCl, 1 mM 3-sialyl-lactose as donor, 1 mM *N*-acetylglucosamine were incubated with purified 300 ng *trans*-sialidase enzyme of *T. cruzi* [46] or 15 min at room temperature. Samples were diluted about 12 times with deionized water and analyzed by high-performance anion-exchange chromatography with pulsed amperometric detection (HPAEC-PAD). The percentage inhibition of TcTS enzyme was calculated from the amount of 3'-sialyl-*N*-acetylglucosamine as compared to total

amount of sialylated compounds in the presence or absence of tested compounds. All compounds were dissolved in DMSO (10 mM), and 2 μ L of these was used in incubation. The control assay mixture was prepared in absence of tested compounds, was performed accordingly by adding the 2 μ L of DMSO to incubated mixture [47,48].

4.4.2. Analysis by HPAEC-PAD

The Dionex ICS 5000 HPLC system was used, which was equipped with the pulsed amperometric detector, carboPac PA-100 ion exchange analytical column (4 \times 250 mm) and PA-100 guard column (4 \times 50 mm). The 80 mM NaOH with a linear gradient from 0 to 500 mM NaAcO was used for elution, at a flow rate of 0.9 mL/min within 60 min.

Funding

We wish to express our gratitude to the Consejo Nacional de Ciencia y Tecnología, Mexico (Proyecto Apoyado por el Fondo Sectorial de Investigación para la Educación, CB-2014-01, 241615) and Secretaría de Investigación y Posgrado del Instituto Politécnico Nacional (SIP-20180306) for their financial support.

Acknowledgements

Muhammad Kashif is the recipient of a scholarship (No. 590887/715369) from Consejo Nacional de Ciencia y Tecnología, Mexico. Gildardo Rivera, Alicia Reyes-Arellano, Esther Ramírez-Moreno and Benjamín Noguera-Torres hold a scholarship from the "Comisión de Operación y Fomento de Actividades Académicas" (COFAA-IPN) and the "Programa de Estímulos al Desempeño de los Investigadores" (EDI-IPN). We thank Oscar Competella and his group from the Universidad Nacional General San Martín (UNSAM) Argentina, for their kind gift of trans-sialidase from *T. cruzi*. Support for this work from the Universidad de Buenos Aires, the CONICET and the ANPCyT is gratefully acknowledged. RA and MLU are research members of the CONICET.

Appendix A. Supplementary data

Supplementary data related to this article can be found at <https://doi.org/10.1016/j.ejmech.2018.07.005>.

References

- [1] C. Chagas, Nova tripanozomíaze humana: estudos sobre a morfologia e o ciclo evolutivo do Schizotrypanum cruzi, n. sp., agente etiológico de nova entidade morbidada homem, Mem. Inst. Oswaldo Cruz 1 (1909) 159–218.
- [2] A. Cruz-Reyes, J.M. Pickering-Lopez, Chagas disease in Mexico: an analysis of geographical distribution during the past 76 years—a review, Mem. Inst. Oswaldo Cruz 101 (2006) 345–354.
- [3] J.R. Coura, J.C. Dias, Epidemiology, control and surveillance of Chagas disease: 100 years after its discovery, Mem. Inst. Oswaldo Cruz 104 (2009) 31–40.
- [4] C.J. Salomon, First century of Chagas' disease: an overview on novel approaches to nifurtimox and benznidazole delivery systems, J. Pharmacol. Sci. 101 (2012) 888–894.
- [5] J.A. Castro, M.M. deMecca, L.C. Bartel, Toxic side effects of drugs used to treat Chagas' disease (American trypanosomiasis), Hum. Exp. Toxicol. 25 (2006) 471–479.
- [6] R. Viotti, C. Vigliano, B. Lococo, M.G. Alvarez, M. Petti, G. Bertocchi, A. Armenti, Side effects of benznidazole as treatment in chronic Chagas disease: fears and realities, Expert Rev. Anti Infect. Ther. 7 (2009) 157–163.
- [7] J. Altcheh, G. Moscatelli, S. Moroni, G.F. Bourmissen, H. Freilij, Adverse events after the use of benznidazole in infants and children with Chagas disease, Pediatrics 127 (2011) 212–218.
- [8] V.P. Santos, E.S. Barrias, J.F. Santos, T.L. Barros Moreira, T.M. De Carvalho, J.A. Urbina, W. De Souza, Effects of amiodarone and posaconazole on the growth and ultrastructure of Trypanosoma cruzi, Int. J. Antimicrob. Agents 40 (2012) 61–71.
- [9] N. Chamond, N. Coatnoan, P. Minoprio, Immunotherapy of Trypanosoma cruzi infections, Curr. Drug Targets - Immune, Endocr. Metab. Disord. 2 (2002) 247–254.
- [10] A. Buschiazzo, M.F. Amaya, M.L. Cremona, A.C. Frasch, P.M. Alzari, The crystal structure and mode of action of trans-sialidase, a key enzyme in Trypanosoma cruzi pathogenesis, Mol. Cell 31 (2002) 757–768.
- [11] M.F. Amaya, A.G. Watts, I. Damager, A. Wehenkel, T. Nguyen, A. Buschiazzo, G. Paris, A.C. Frasch, S.G. Withers, P.M. Alzari, Structural insights into the catalytic mechanism of Trypanosoma cruzi trans-sialidase, Structure 31 (2004) 775–784.
- [12] S. Buchini, A. Buschiazzo, S.G. Withers, A new generation of specific Trypanosoma cruzi trans-sialidase inhibitors, Angew. Chem. Int. Ed. 25 (2008) 2700–2703.
- [13] M. Kashif, A.M. Herrera, E.E. Lara-Ramirez, E. Ramirez-Moreno, V.B. Garcia, M. Ashfaq, G. Rivera, Recent developments in trans-sialidase inhibitors of Trypanosoma cruzi, J. Drug Target. 25 (2017) 485–498.
- [14] A.H. Lima, J. Lameira, C.N. Alves, Protein–ligand interaction of T. cruzi trans-sialidase inhibitors: a docking and QM/MM MD study, Struct. Chem. 1 (2012) 147–152.
- [15] J. Neres, P. Bonnet, P.N. Edwards, P.L. Kotian, A. Buschiazzo, P.M. Alzari, K.T. Douglas, Benzoic acid and pyridine derivatives as inhibitors of Trypanosoma cruzi trans-sialidase, Bioorg. Med. Chem. 15 (2007) 2106–2119.
- [16] J. Neres, M.L. Brewer, L. Ratier, H. Botti, A. Buschiazzo, P.N. Edwards, P.N. Mortenson, M.H. Charlton, P.M. Alzari, A.C. Frasch, R.A. Bryce, Discovery of novel inhibitors of Trypanosoma cruzi trans-sialidase from in silico screening, Bioorganic Med. Chem. Lett 1 (2009) 589–596.
- [17] J.H. Kim, H.W. Ryu, J.H. Shim, K.H. Park, S.G. Withers, Development of new and selective trypanosoma cruzi trans-sialidase inhibitors from sulfonamide chalcones and their derivatives, Chembiochem 12 (2009) 2475–2479.
- [18] S. Arioka, M. Sakagami, R. Uematsu, H. Yamaguchi, H. Togame, H. Takemoto, H. Hinou, S.I. Nishimura, Potent inhibitor scaffold against Trypanosoma cruzi trans-sialidase, Bioorg. Med. Chem. 15 (2010) 1633–1640.
- [19] M. Kashif, A. Moreno-Herrera, J.C. Villalobos-Rocha, B. Noguera-Torres, J. Pérez-Villanueva, K. Rodríguez-Villar, G. Rivera, Benzoic acid derivatives with trypanocidal activity: enzymatic analysis and molecular docking studies toward trans-sialidase, Molecules 22 (2017) 1863.
- [20] T. Noguchi, R. Shimazawa, K. Nagasawa, Y. Hashimoto, Thalidomide and its analogues as cyclooxygenase inhibitors, Bioorganic Med Chem Lett 12 (2002) 1043–1046.
- [21] H. Sano, T. Noguchi, A. Tanatani, Y. Hashimoto, H. Miyachi, Design and synthesis of subtype-selective cyclooxygenase (COX) inhibitors derived from thalidomide, Bioorg. Med. Chem. 13 (2005) 3079–3091.
- [22] A.M. Alaa, K.E. ElTahir, Y.A. Asiri, Synthesis, anti-inflammatory activity and COX-1/COX-2 inhibition of novel substituted cyclic imides. Part 1: molecular docking study, Eur. J. Med. Chem. 46 (2011) 1648–1655.
- [23] A.M. Alaa, A.S. El-Azab, S.M. Attia, A.M. Al-Obaid, M.A. Al-Omar, H.I. El-Subbagh, Synthesis and biological evaluation of some novel cyclic-imides as hypoglycaemic, anti-hyperlipidemic agents, Eur. J. Med. Chem. 46 (2011) 4324–4329.
- [24] A.M. Alanazi, A.S. El-Azab, I.A. Al-Suwaidan, K.E. ElTahir, Y.A. Asiri, N.I. Abdel-Aziz, A.M. Alaa, Structure-based design of phthalimide derivatives as potential cyclooxygenase-2 (COX-2) inhibitors: anti-inflammatory and analgesic activities, Eur. J. Med. Chem. 92 (2015) 115–123.
- [25] A.A.M. Abdel-Aziz, A.S. El-Azab, S.M. Attia, A.M. Al-Obaid, M.A. Al-Omar, H.I. El-Subbagh, Synthesis and biological evaluation of some novel cyclicimides as hypoglycaemic, anti-hyperlipidemic agents, Eur. J. Med. Chem. 46 (2011) 4324–4329.
- [26] A.M. Alanazi, A.S. El-Azab, I.A. Al-Suwaidan, K.E.H. ElTahir, Y.A. Asiri, N.I. Abdel-Aziz, Structure-based design of phthalimide derivatives as potential cyclooxygenase-2 (COX-2) inhibitors: anti-inflammatory and analgesic activities, Eur. J. Med. Chem. 92 (2015) 115–123.
- [27] A.A.M. Abdel-Aziz, A.S. El-Azab, S.M. Attia, A.M. Al-Obaid, M.A. Al-Omar, H.I. El-Subbagh, Synthesis and biological evaluation of some novel cyclicimides as hypoglycaemic, anti-hyperlipidemic agents, Eur. J. Med. Chem. 46 (2011) 4324–4329.
- [28] K. Kamiński, J. Obniska, B. Wiklik, D. Atamanyuk, Synthesis and anticonvulsant properties of new acetamide derivatives of phthalimide, and its saturated cyclohexane and norbornene analogs, Eur. J. Med. Chem. 46 (2011) 4634–4641.
- [29] H. Akgün, I. Karamelekoğlu, B. Berk, I. Kurnaz, G. Sarıbiyik, S. Öktem, Synthesis and antimicrobial activity of some phthalimide derivatives, Bioorg. Med. Chem. 20 (2012) 4149–4154.
- [30] R. Williams, J.T. Manka, A.L. Rodriguez, P.N. Vinson, C.M. Niswender, C.D. Weaver, Synthesis and SAR of centrally active mGlu5 positive allosteric modulators based on an aryl acetylenic bicyclic lactam scaffold, Bioorg. Med. Chem. Lett 21 (2011) 1350–1353.
- [31] M.V.D.O. Cardoso, D.R.M. Moreira, G.B.O. Filho, S.M.T. Cavalcanti, L.C.D. Coelho, J.W.P. Espindola, Design, synthesis and structure–activity relationship of phthalimides endowed with dual antiproliferative and immunomodulatory activities, Eur. J. Med. Chem. 96 (2015) 491–503.
- [32] C. Pessoa, P.M.P. Ferreira, L.V.C. Lotufo, M.O. de Moraes, S.M.T. Cavalcanti, L.C.D. Coelho, Discovery of phthalimides as immunomodulatory and anti-tumor drug prototypes, ChemMedChem 5 (2010) 523–528.
- [33] P.M. da Costa, M.P. da Costa, A.A. Carvalho, S.M.T. Cavalcanti, M.V. de Oliveira Cardoso, G.B. de Oliveira Filho, Improvement of in vivo anticancer and anti-angiogenic potential of thalidomide derivatives, Chem. Biol. Interact. 239 (2015), 74–183.

- [34] E.F. de Santiago, S.A. de Oliveira, G.B. de Oliveira Filho, D.R.M. Moreira, P.A.T. Gomes, A.C.L.A.C.L. da Silva, Evaluation of the anti-schistosoma mansoni activity of thiosemicarbazones and thiazoles, *Antimicrob. Agents Chemother.* 58 (2014) 352–363.
- [35] P.A. de Moraes Gomes, A.R. Oliveira, M.V. de Oliveira Cardoso, E. de Farias Santiago, M. de Oliveira Barbosa, L.R. de Siqueira, D.R. Moreira, T.M. Bastos, F.A. Brayner, M.B. Soares, A.P. de Oliveira Mendes, Phthalimido-thiazoles as building blocks and their effects on the growth and morphology of *Trypanosoma cruzi*, *Eur. J. Med. Chem.* 23 (2016), 46–5.
- [36] A.V. Lebedev, A.B. Lebedeva, V.D. Sheludyakov, E.A. Kovaleva, O.L. Ustinova, I.B. Kozhevnikov, Competitive formation of β -amino acids, propenoic, and ylidenemalonic acids by the rodionov reaction from malonic acid, aldehydes, and ammonium acetate in alcoholic medium, *Russ. J. Gen. Chem.* 75 (2005) 1113–1124.
- [37] M. Ashfaq, Synthesis of novel bioactive phthalimido-4-methyl pentanoateorganotin (IV) esters with spectroscopic investigation, *J. Organomet. Chem.* 691 (2006) 1803–1808.
- [38] A.G. Watts, I. Damager, M.L. Amaya, A. Buschiazzi, P. Alzari, A.C. Frasch, S.G. Withers, *Trypanosoma cruzi* trans-sialidase operates through a covalent sialyl-enzyme intermediate: tyrosine is the catalytic nucleophile, *J. Am. Chem. Soc.* 125 (2003) 7532–7533.
- [39] A.R. Todeschini, L. Mendonça-Previato, J.O. Previato, A. Varki, H.V. Halbeek, Trans-sialidase from *Trypanosoma cruzi* catalyzes sialoside hydrolysis with retention of configuration, *Glycobiology* 10 (2000) 213–221.
- [40] R. Agustí, G. París, L. Ratier, A.C.C. Frasch, R.M. de Lederkremer, Lactose derivatives are inhibitors of *Trypanosoma cruzi* trans-sialidase activity toward conventional substrates in vitro and in vivo, *Glycobiology* 14 (2004) 659–670.
- [41] G.M. Morris, R. Huey, W. Lindstrom, M.F. Sanner, R.K. Belew, D.S. Goodsell, A.J. Olson, AutoDock4 and AutoDockTools4: automated docking with selective receptor flexibility, *J. Comput. Chem.* 16 (2009) 2785–2791.
- [42] O. Trott, A.J. Olson, AutoDock Vina: improving the speed and accuracy of docking with a new scoring function, efficient optimization, and multi-threading, *J. Comput. Chem.* 31 (2010) 455–461.
- [43] Dassault Systèmes BIOVIA, Discovery Studio Modeling Environment, Release 2017, Dassault Systèmes, San Diego, 2016.
- [44] C. Mendoza-Martínez, J. Correa-Basurto, R. Nieto-Meneses, A. Márquez-Navarro, R. Aguilar-Suárez, M.D. Montero-Cortés, B. Noguera-Torres, E. Suárez-Contreras, N. Galindo-Sevilla, Á. Rojas-Rojas, A. Rodríguez-Lezama, Design, synthesis and biological evaluation of quinazoline derivatives as anti-trypanosomatid and anti-plasmodial agents, *Eur. J. Med. Chem.* 96 (2015) 296–307.
- [45] Z. Brener, Therapeutic activity and criterion of cure on mice experimentally infected with *Trypanosoma cruzi*, *Rev. Inst. Med. Trop. Sao Paulo* 6 (1962) 389–396.
- [46] J.C. Villalobos-Rocha, L. Sánchez-Torres, B. Noguera-Torres, A. Segura-Cabrera, C.A. García-Pérez, V. Bocanegra-García, I. Palos, A. Monge, G. Rivera, Anti-*Trypanosoma cruzi* and anti-leishmanial activity by quinoxaline-7-carboxylate 1, 4-di-N-oxide derivatives, *J. Parasitol. Res.* 113 (2014) 2027–2035.
- [47] A. Buschiazzi, A.C. Frasch, O. Campetella, Medium scale production and purification to homogeneity of a recombinant trans-sialidase from *Trypanosoma cruzi*, *Cell. Mol. Biol.* 42 (1996) 703–710.
- [48] M.E. Cano, R. Agustí, A.J. Cagnoni, M.F. Tesoriero, J. Kovensky, M.L. Uhrig, R.M. de Lederkremer, Synthesis of divalent ligands of β -thio- and β -N-galactopyranosides and related lactosides and their evaluation as substrates and inhibitors of *Trypanosoma cruzi* trans-sialidase, *Beilstein J. Org. Chem.* 10 (2014) 3073.